COMPREHENSIVE PNEUMOLOGY CENTER (CPC),
HELMHOLTZ ZENTRUM MÜNCHEN,
LUDWIG-MAXIMILIANS-UNIVERSITÄT
MÜNCHEN

Dissertation for the awarding of a Doctor of Philosophy
(Ph.D.)
at the Medical Faculty of the
Ludwig-Maximilians-Universität München

Harnessing Adeno Associated Virus (AAV) Technology for the Treatment of Scarring

Submitted by:

Vijayanand Rajendran

Sivagangai, India

2021

Mit freundlicher Genehmigung der Ludwig-Maximilians-Universität München

First evaluator**:** **Dr. Yuval Rinkevich**

Second evaluator**:** **PD Dr.Claudia Staab-Weijnitz**

Third evaluator**:** **Prof. Dr. med.Jürgen Behr**

Fourth evaluator**:** **Prof. Dr. med. Gerd Gauglitz**

Dean: **Prof. Dr. med. Thomas Gudermann**

Date of Oral Defense**:** **03.06.2022**

TABLE OF CONTENTS

ABSTRACT

Deep skin wounds rapidly heal with scars and contractures by mobilizing extracellular matrix and cells from the fascia, deep beneath the dermal layer of the skin. Here, we demonstrate that adeno-associated virus 8 (AAV8) is highly effective for transducing scar-forming fibroblasts in the fascia. p120 is up-regulated explicitly in scar-forming fibroblasts populations in response to injury. We demonstrate in animals that AAV8 mediated short hairpin RNA (ShRNA) silencing of p120, specifically in the fascia, reduces extracellular matrix (ECM) mobilization and enables scarless wound repair outcomes. Our findings demonstrate the potential for specifically targeting mechanisms of fascia mobilization with AAV8 vectors and the translational applications of this technology in modulating endogenous repair responses to restore the function of injured tissues in a scarless fashion.

INTRODUCTION

1.1 Scarring

Tissue injury can have a variety of diverse consequences, ranging from scarring to regeneration[1]. After the injury, the most favourable outcome would be regenerating a perfect replica of the original tissue foundation, form and function, occurring in flatworms and sea squirts[2]. However, regeneration of mammalian skin that follows injury is uncommon, and skin frequently heals inadvertently by scar tissue deposition and tissue contraction, resuming its primary function as an exterior barrier without regaining its original architecture[3]. Although scarring frequently assures the organism's survival, scarring is unpleasant and impairs tissue function. Scientists have attempted to harness regeneration in humans for over a century, taking inspiration from the whole-body regeneration of lower vertebrates. Skin scarring generally resulting from burns or surgical interventions imposes an enormous hardship on individuals. Many people with significant scars, especially children, may suffer from lifelong physical dysfunction and mental distress [4],[5]. Approximately 500,000 people undergo burn treatments every year in the United States alone; many of them suffer severe scarring and contractures with functional problems [6]. An estimated $7.5 billion is spent yearly on burn treatment, the majority of which is devoted to treating the scar [7]. In developed countries, over 100 million people annually develop scars due to surgical procedures. Patients with noticeable scars, particularly on the face, may experience psychological trauma and social problem [8],[9]. Overall, scarring is a tremendous burden onpatients and healthcare systems and is an unmet clinical problem.

1.2 Anatomy of the Skin

Skin is an intricated structure comprising many layers, each with multiple functions (**Figure 1A, B**). The upper layer or epidermis serves as a protective barrier against trans-epidermal water loss. Keratinocytes account for 95% of total cells residing in the epidermis. Other epidermal cells include melanocytes (pigment production), Langerhans cells (immune function) and Merkel cells (sensory)[10],[11]. The epidermis layer below is called the dermis, which provides nutrients to the non-vascularised epidermis.

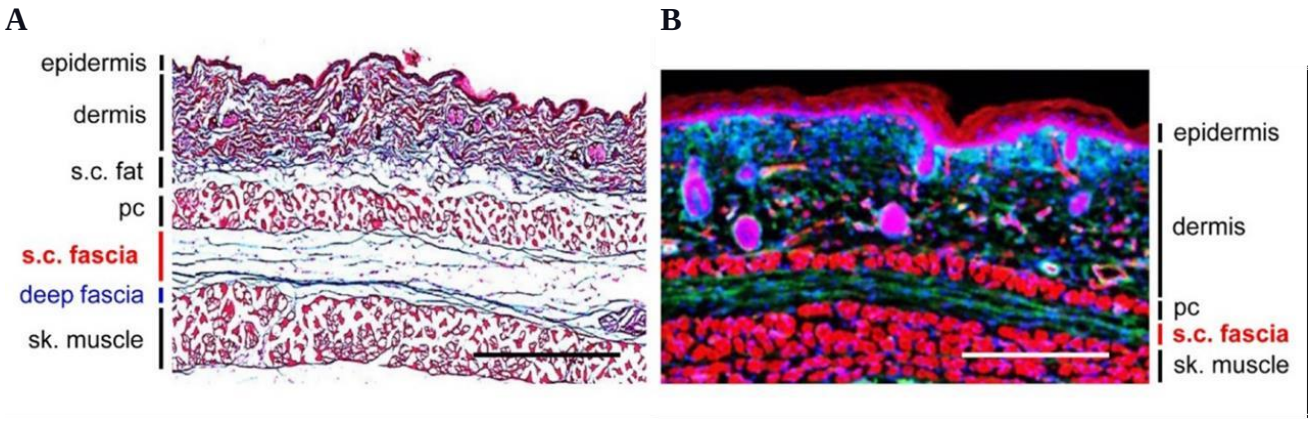

Figure 1: Anatomy of mouse skin (**A**) Masson trichrome of uninjured mouse skin showing epidermis, dermis, panniculus carnosus (pc), subcutaneous (s.c) fat, subcutaneous (s.c) fascia, deep fascia, skeletal (sk) muscle. Collagen in the dermis and fascia are stained in blue. (**B**) Immunofluorescence staining of back skin from En1Cre; R26mTmG showing scar-forming fibroblasts (GFP) known as Engrailed-1 lineage positive fibroblasts (EPF)

Skin's dermis is responsible for flexibility and strength. The dermis is mainly composed of fibroblasts, including macrophages and mast cells. The dermis consists of sensory nerve ends, hair follicles, blood vessels, and secretory glands[11]. The subcutaneous fat layer is present underneath the dermis, where fat is stored in adipose cells, and the fat layer is responsible for energy storage and thermal insulation[12]. The fascia layer lies beneath the adipose and the muscle layer (*panniculus carnosus)*. Fascia is crucial for maintaining the

integrity of the skin and supporting a number of structures, including lymphatic vessels, adipose tissue and nerve fibres. Fascia consists of loosely woven collagen fibers representing its structure's elastic nature. A significant cellular component of fascia comprises fibroblasts, adipocytes, pericytes, and immune cells such as lymphocytes and macrophages[13].

1.3 Stages of Wound Healing and Scarring Process

The wound healing process is classified into four stages: hemostasis, inflammation, proliferation, and remodelling (**Figure 2**). The platelets activation and fibrin clot formation in the wounded space prevent bleeding, providing hemostasis and triggering the inflammatory process [15],[16]. The activation of platelets mediate the secretion of different chemical mediators and growth factors, including transforming growth factor (TGF)-β, fibroblast growth factor (FGF), interleukin 8 (IL-8), platelet-derived growth factor (PDGF),and epidermal growth factor (EGF)[16]. Thrombin activation and the release of several chemical mediators from mast cells increase vasodilation, blood flow, and facilitate inflammatory cells' migration and promote the inflammatory process, which is highlighted by successive infiltration of neutrophils, macrophages and lymphocytes. Neutrophils are the first inflammatory cells that migrate into the wound site[17]. Neutrophils are phagocytic that kill bacteria and degrade other foreign materials[18]– [20]. In addition, neutrophils secrete several chemical mediators, including tumour necrosis factor (TNF), interleukin-6 (IL-6), which contribute to the inflammatory response[22],[23].

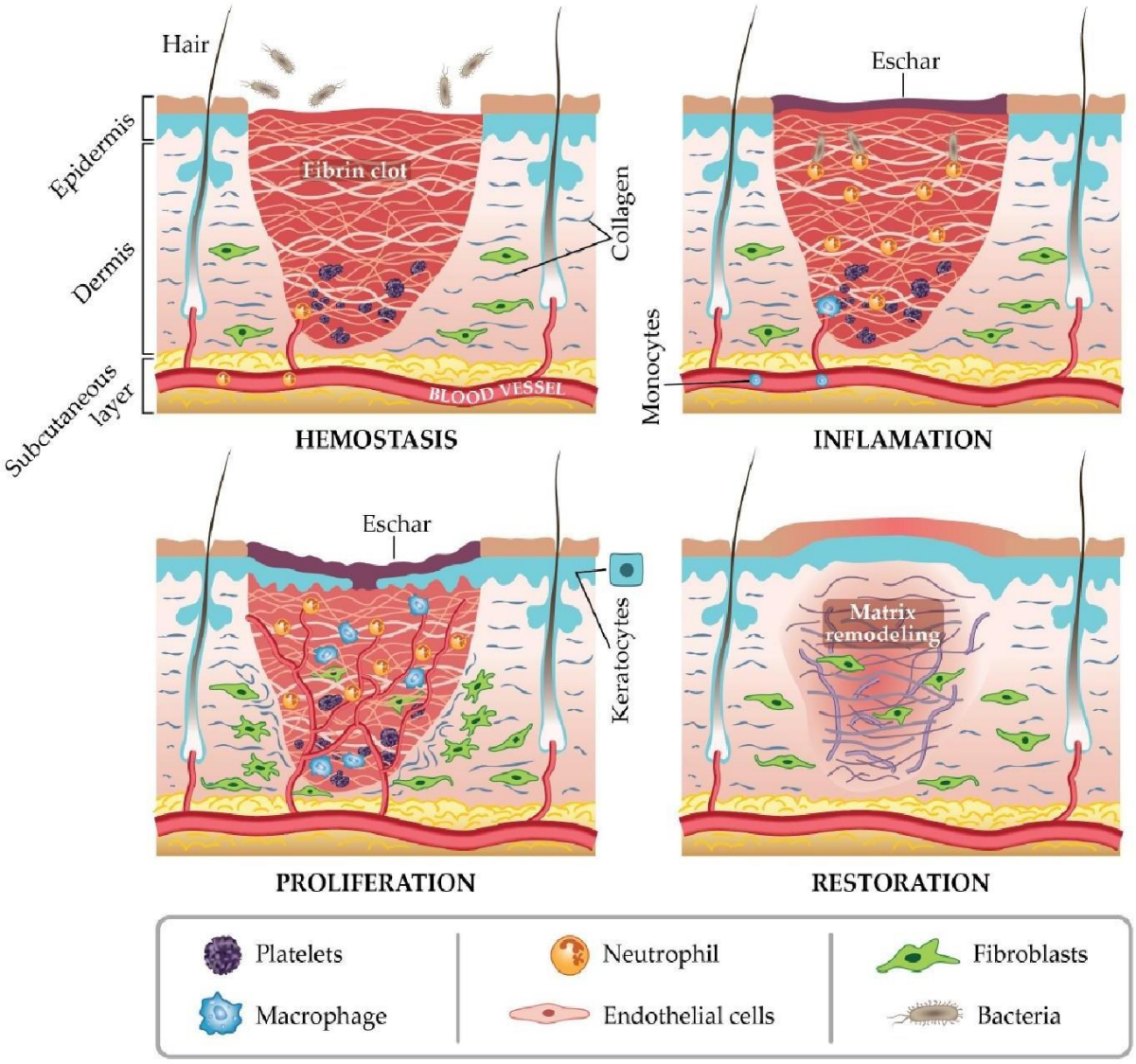

Figure 2: Schematics describing the four stages of wound healing. 1) Hemostasis: Fibrin clot formation and neutrophil requirement 2) Inflammation: Neutrophil and Macrophage requirement 3) Proliferation: Re-epithelization, angiogenesis and granular tissue formation 4) Wound Closure, and matrix remodelling (type I Collagen deposition).

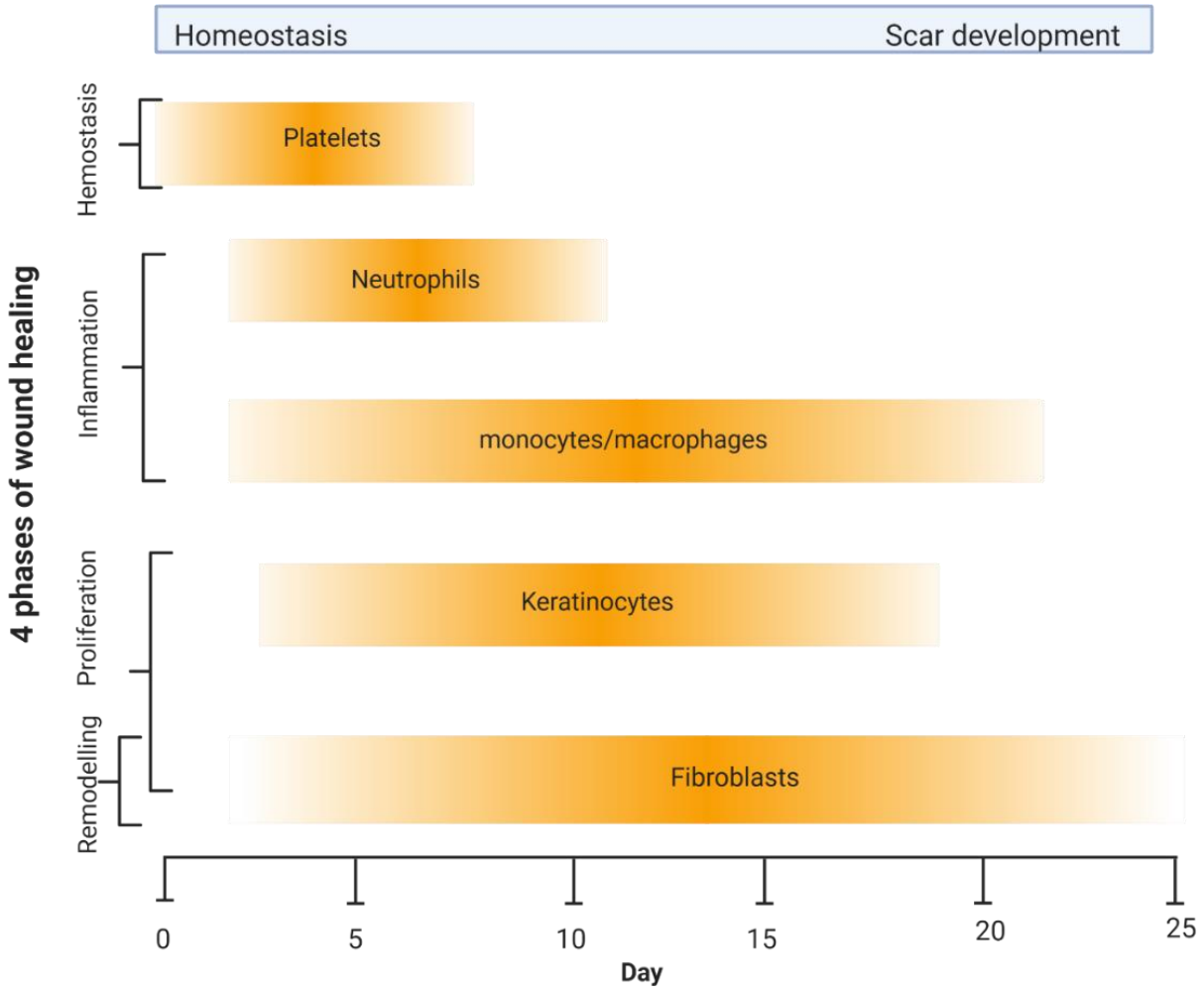

Figure 3: Schematic representation of key cellular players in the different stages of wound healing.

After 24–48 hours, the number of neutrophils peaks, and monocytes are the primary inflammatory cells in the wound[23]. Mast cells release monocyte chemoattractant protein-1 (MCP-1), which influx the monocytes into the wound bed, where they differentiate into macrophages[24]. The wound macrophages promote angiogenesis and granulation tissue formation by releasing chemical mediators such as PDGF, VEGF, and TGFβ. Macrophages assist in inducing and clearing apoptotic including neutrophils from the injury sites, thus facilitating wound inflammation resolution[25]. Around 72 hours after injury, the inflammatory

phase of the wound ends and the wound enters into the proliferative phase. The proliferative phase (which lasts between 2 and 10 days following injury) is responsible for granulation tissue formation to fill the wound. Fibroblasts are mesenchymal cells that play a significant role in skin integrity by proliferating, differentiating, and coordinating with other cells both in homeostasis and disease states, irrespective of the nature of skin injury[26]. Once the inflammation diminishes, proliferation takes over to close the wound, including re-epithelisation, angiogenesis, and granulation tissue formation. The re-epithelialization of the injury involves the migration and proliferation of keratinocytes. There are various signals, cytokines, and growth factors, which can trigger re-epithelialisation, including epidermal growth factor (EGF), insulin growth factor-1 (IGF-1)and keratinocyte growth factor (KGF) [27]. During the proliferation phase, the fibrin-based provisional wound matrix formed during the haemostasis is substituted by granulation tissue[28]. Fibroblasts play a central role in the formation of granulation tissue. In response to chemical mediators such as PDGF, TGF-β, fibroblasts migrate into the provisional wound matrix[29], [30].

Fibroblasts are the central cells responsible for the deposition of collagen and other extracellular matrix (ECM) components, ultimately filling up the wound gap[31]. The remodelling phase begins at the end of granulation tissue formation. TGF-β triggers the transition of fibroblasts into alpha-smooth muscle actin (α-SMA) expressing myofibroblasts[32]. At this stage, type I collagen, which has greater tensile strength, progressively substitutes the pre-existing type III collagen[33]. The hallmark of a scar is the accumulation of abnormally structured ECM within a wound. In the final stage, collagen in scar tissue becomes thicker and parallel with superior tensile strength[34]. In scar development, myofibroblasts are the primary producers of the extracellular matrix.

1.4 Role of the Fascia in Wound Closure and Scarring

According to new studies [35]–[37], deep skin injuries cause the subcutaneous fascia to move into the wounds, generating the provisional wound matrix (**Figure 3**). The mobilised fascia drags the extracellular matrix along with fibroblasts into the wound. It also contains blood vessels, macrophages, and peripheral nerves, crucial in wound healing[35]. The provisional matrix derived from the fascia matrix attracts the inflammatory cells. The fascia mobilisation is directed by fascia resident fibroblasts known as Engrailed-1 lineage positive fibroblasts (EPF) that deposit extensive ECM and contribute to scarring. According to our recent study, fascia resident EPFs collectively migrate into the wound in response to the injury. The ablation of fascial residents fibroblasts reduced the matrix integration into the wound, leading to scar severity reduction[35]. In addition, cell adhesion molecule N-cadherin and Gap junction protein connexin-43 were selectively expressed at the higher level in fascial fibroblast upon injury. Inhibition of N-cadherin or connexin-43 potentially reduces the fascial mobilisation and collagen deposition in wounds [36], [37]. These results show that scarring may be minimised by targeting the fascial fibroblasts. It is worth investigating this new approach to gain better insights into the pathophysiology of scarring.

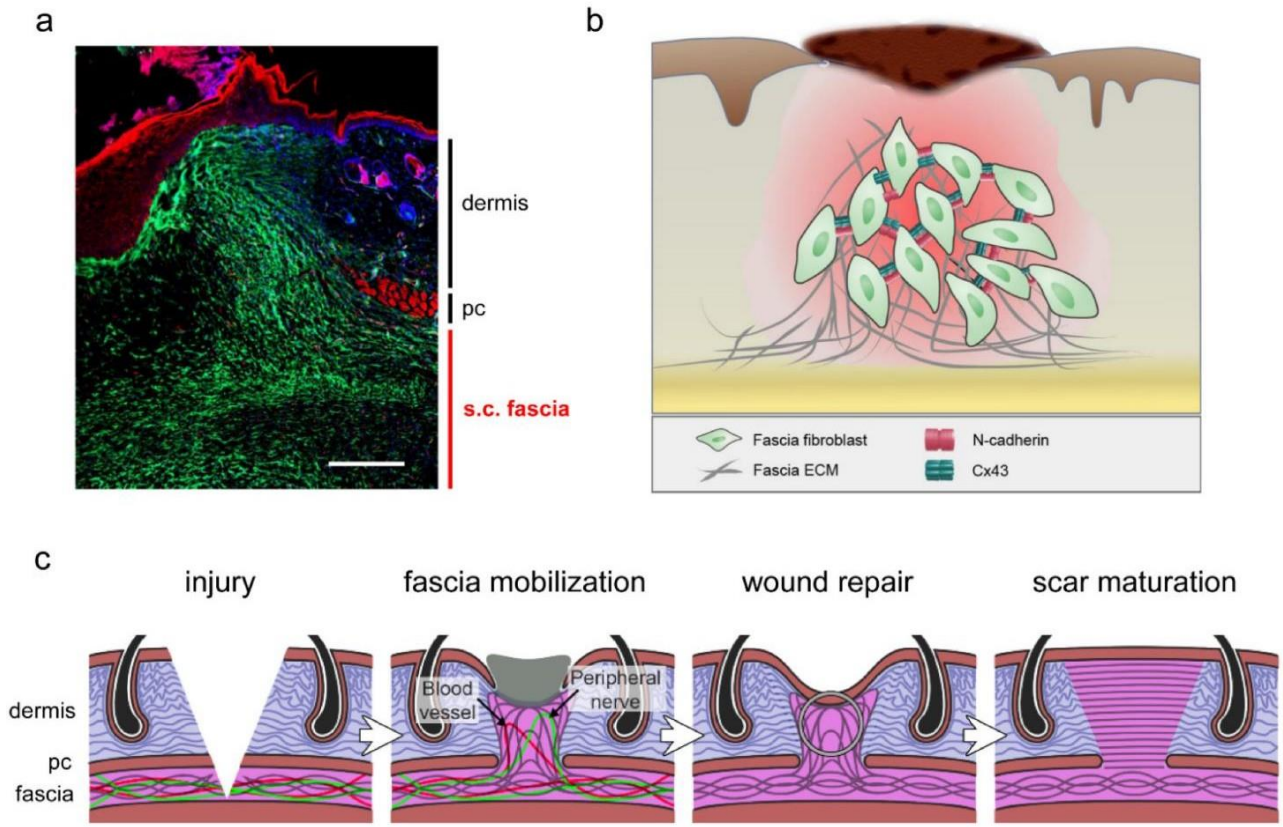

Figure 3: Wound repair by subcutaneous fascia. (**A**) En1Cre; R26mTmG transgenic mice demonstrating fascia residing fibroblasts are directed into wounds at 7 days post-wound pc, panniculus carnosus; s.c., subcutaneous. (**B**) The collective migration of fascial fibroblasts is associated with the upregulation of N-cadherin and Connexin 43. (**C**) Fascial fibroblasts mobilize the fascial matrix to seal wounds, commence wound healing, and generate mature scars.

1.5 Characteristics of Scar

All scarring primarily comprises an excessive amount of collagen compared to normal skin. Scarring consists higher proportion of type I collagen (80-90%). In contrast, type III collagen is present in more significant quantities in normal skin [33]. Scar tissue shows distinct characteristics such as distortion of the orientation of collagen fibers, lack of dermal appendages and the modification of skin texture (**Figure 4**). Collagen in normal skin forms basket weave orientation, whereas collagen bundles show parallel alignment in the scar tissue [30].

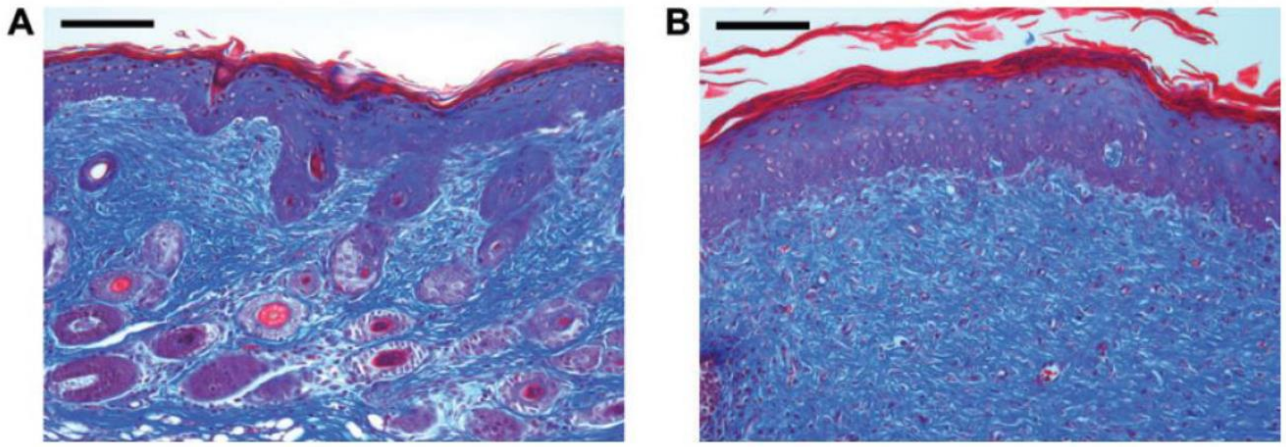

1.6 The spectrum of skin scar types

Abnormal scars can be classified based on the dynamic balance of the tissue during scar formation and regeneration. Additional factors such as type of injury, anatomical location, severity and depth of the scar, genetic susceptibility, sex, and environmental factors also contribute to the following scar types.

Widespread scars, known as 'stretched scars', are typical after surgery. Scar formation occurs when the surgical incision line progressively expands and stretch over time. Pregnancy stretch marks in the abdomen are widespread scars. Stretch marks are caused

by dermal injury due to mechanical stress in the connective tissue. It usually appears as a flat, pale, soft scar after knee or shoulder surgeries. As the scars mature, they do not show elevation, thickening, or nodules, which differentiates mature widespread scars from hypertrophic scars[38].

Hypertrophic scars (HTS) are defined as elevated scars that stay within the confines of the initial lesion, and, in most cases, these scares tend to regress on their own. Hypertrophic scars are pink or red. These scars can be painful and itchy[39].

Contracture scars occur due to a contractile wound-healing process that forms mainly after a burn that results in a loss of a larger area of skin. The scar formation pulls the edges of the skin together, often resulting in physical deformities and movement restriction[38].

Keloid scars are raised scars that spread beyond the initial wound's edges and infiltrate the surrounding normal skin. A keloid scar continues to expand over time, does not subside on its own, and shows a high recurrence rate [39].

1.7 Traditional and Current Treatment Approaches to Scarring

Traditional scar-reduction strategies employed by surgeons include performing the surgical incision along with Langer's lines and deep dermal sutures to reduce the tension on wound edges [40]. Simple paper tape is placed on the healing wounds to prevent hypertrophic scar formation[41]. The scarring has been treated with silicone gel sheets (SGS). However, clinical investigations proved that SGS had not significantly improved hypertrophic and keloid scars[42]. Onion extracts are available in the form of dressings and gels. The flavonoids may limit fibroblast growth and collagen synthesis, reducing excessive scar formation[43]. However, the clinical study on the efficacy of onion extract to prevent the keloid and hypertrophic scars remains inconsistent. Intralesional injections of corticosteroids are the standard treatment options for keloids. Corticosteroids suppress the inflammatory response that occurs in the scar tissue. According to several trials, most patients improve their keloid without relapse after steroid injection[44]. A pressure garment is a widely used treatment for burn scars. However, many anatomic areas cannot be successfully covered by pressure garments. Patients find it very distressing to wear these garments for long periods[45] Moreover, the mechanisms of pressure treatment have not been fully understood yet. Laser therapy has been employed to enhance scar appearance with variable effectiveness[42]. 585nm pulsed dye laser (PDL) causes intravascular coagulation, which destroys the microvascular network and reduces the expression of proinflammatory mediators such as TGF-β1[46]. Thus, according to the recent guidelines, PDL should be used in the first- or second-line treatment of immature hypertrophic scars. Ablative laser procedures show promising results in treating the extensive hypertrophic scar. On the other hand, ablative lasers do not provide any benefits in treating keloids[47]. Imiquimod 5% cream (Aldara) regulates the immune response and improves healing. It has been used to treat the keloid occurrence after the surgery[48]. However, patients showed recurrence of keloids, indicating

the drug's impact in treating the keloids is limited. There has been a minimal success with administering several other injectable and topical medications, including immune modulators, hyaluronidase, and cell-based therapy[30], [47]. Surgical revisions are often necessary for these patients as a last resort. In recent years, several new medicines have been evaluated in humans for their effectiveness in treating scarring and other fibrotic diseases. Metelimumab (CAT-192) is a human IgG4 monoclonal antibody (mAb) that suppresses transforming growth factor-beta β (TGF-β). It was ineffective in treating scleroderma and was withdrawn from clinical trials[49]. Imatinib mesylate, an inhibitor of PDGF-R, was also unsuccessful in treating scleroderma skin fibrosis[50]. After completing phase I/II studies, human recombinant TGF-β3 (Avotermin) failed to meet the Phase III scarring treatment study[51]. The findings of a clinical trial exploring the use of dermal fibroblasts to treat burn scars have not been published[52]. In phase II trials, the antisense nucleotide EXC 001, which inhibits connective tissue growth factor (CTGF), showed promising results[53]. However, the current status of this drug is not available to the public.

1.8 AAV Biology

Adeno-associated viruses (AAV) were initially found in a laboratory at the University of Pittsburgh as a simian adenovirus sample [54]. AAVs are small (~ 20 nm in diameter), 4.7-kb single-stranded DNA (ssDNA) and non-enveloped viruses belonging to Dependoparvovirus genus of the Parvoviridae family. AAVs infections were commonly discovered in human blood samples and identified as non-pathogenic viruses[56], [57]. AAVs are low immunogenic, making them an attractive gene delivery technology for various clinical research. AAV genome replication can only occur in co-infecting helper viruses, mainly adenovirus [55]. Its single-stranded DNA genome encodes Rep (Replication), Cap (Capsid) and assembly activating (AAP) proteins. These coding sequences are flanked by inverted terminal repeats (ITRs), containing cis-elements required for replication and packaging[55].

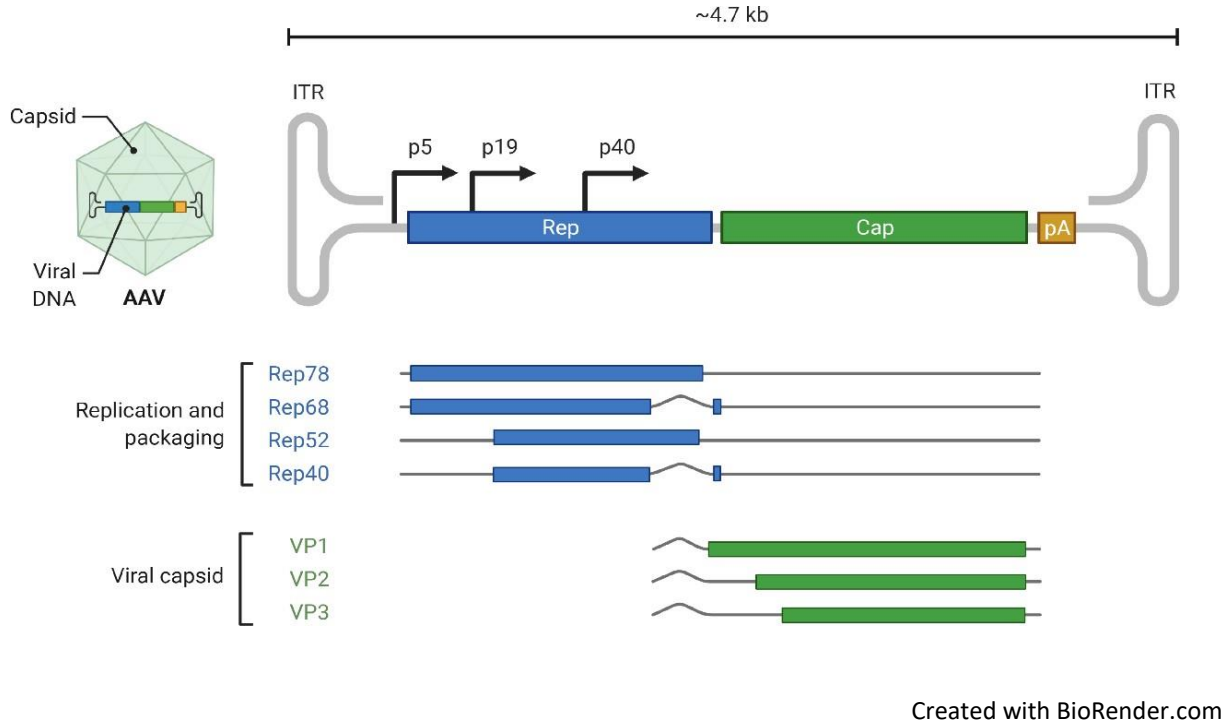

Figure 5: AAV genome. The AAV is approximately 4.7-kilobases (kb) in size. Rep (Replication), Cap (Capsid) and assembly activating (AAP) proteins coding sequences are flanked by inverted terminal repeats (ITRs). Rep genes encode four replication (Rep) proteins (Rep78, Rep68, Rep52, and Rep40). The cap ORF encodes the three capsid proteins VP1, VP2, VP3.

The *Rep* gene encodes four replication isoforms Rep78, Rep68, Rep52, and Rep40. Rep proteins are essential for viral genome replication and packaging. The *cap* (capsid) gene encodes three capsid proteins, isoforms VP1, VP2, and VP3, which self assemble and create the capsid that protects the viral genome[56], [57]. All three capsids proteins are expressed from the p40 promoter due to alternative splicing (AS). The *aap* gene encodes an assembly-activating protein (AAP), which directs capsid proteins to the nucleolus and facilitates the capsid assembly(Figure 5)[58]. The first stage of AAV infection is the attachment to the primary cell surface receptors, followed by the secondary receptor that mediates the cell entry. AAVs bind to the cell surface by interacting with particular glycans or glycoconjugates[59], [60]. AAVs attachment to the host cells depends on their capsids as they differ based on their sequence among serotypes. At least 13 AAV types have been

identified in humans and primates. Each serotype binds to a different surface receptor of the host cell. Each serotype exhibits distinct cell and tissue tropism(Table 1)[60].

Table 1: AAV serotype tropism. It shows receptors information for AAV1-9 and their preferred tissue tropism.

AAV	Primary Receptor	Co-receptor	Tissue tropism
AAV1	N-linked sialic acid	Unknown	Skeletel muscle, CNS, Retina, Pancreas
AAV2	HSPG	FGFR1, HGFR, LamR, CD9	Vascular smoothe muscle, CNS, liver, Kidney, Skeletal muscle
AAV3	HSPG	FGFR1, HGFR, LamR	Skeletal muscle
AAV4	O-linked sialic acid	Unknown	CNS, Retina
AAV5	N-linked sialic acid	PDGFR	Skeletal muscle,CNS, Lung, Retina
AAV6	N-linked sialic acid, HSPG	EGFR	Skeletal muscle, Heart, Lung
AAV7	Unknown	Unknown	Skeletal muscle, Retina, CNS
AAV8	Unknown	LamR	Liver, Skeletal muscle, CNS, Retina, Pancreas, Heart
AAV9	N-linked galactose	LamR	Liver, Heart, Brain, Skeletal muscle, Lungs, Kidney, Pancreas

HSPG, heparan sulfate proteoglycan; FGFR1, fibroblast growth factor receptor 1; HGFR, hepatocyte growth factor receptor; LamR, Laminin receptor; PDGFR, platelet-derived growth factor receptor; EGFR, epidermal growth factor receptor; CNS, central nervous system

1.9 Generation of Recombinant AAV Vectors

The most well-established approach for producing AAV is based on transient co-transfection of 3 plasmids into the host cells, such as HEK293 cells (**Figure 7**). Typically, the first AAV plasmid consists of cis-acting ITRs flanking the foreign gene or non-coding RNAs (cDNAs, ShRNAs, miRNAs), including promoter and poly A sites. The second plasmid carries the Rep and Cap genes. The third plasmid consists of adenoviral helper genes (E2A, E4ORF6 and VA-RNA)[61]–[63]. These plasmids are often transiently co-transfected into HEK-293 cells, then cultured for two to five days before lysing to isolate AAV particles. The additional adenoviral Helper function such as E1A and E2A are already constitutively expressed by HEK-293 cells[64], [65]. The host cell DNA replication machinery converts the single-stranded AAV genome to a transcriptionally active double-stranded DNA and is processed to mRNA. However, it is considered that host cell synthesis of second-strand synthesis represents a significant bottleneck in terms of AAV transduction in post-mitotic cells as DNA replication machinery is inactive in these cells[64]. Self-complementary AAV (scAAV) vectors effectively pass the requirement of host cells second strand synthesis.[66] Recombinant AAV

vectors are designed by replacing rep and cap genes from the wild type AAVs. AAVs' host genomic integration is extremely rare as the recombinant AAV vector lacks the rep gene[66]. AAV vectors have a significant advantage in stable and prolonged gene expression in post-mitotic cells[67], [68].

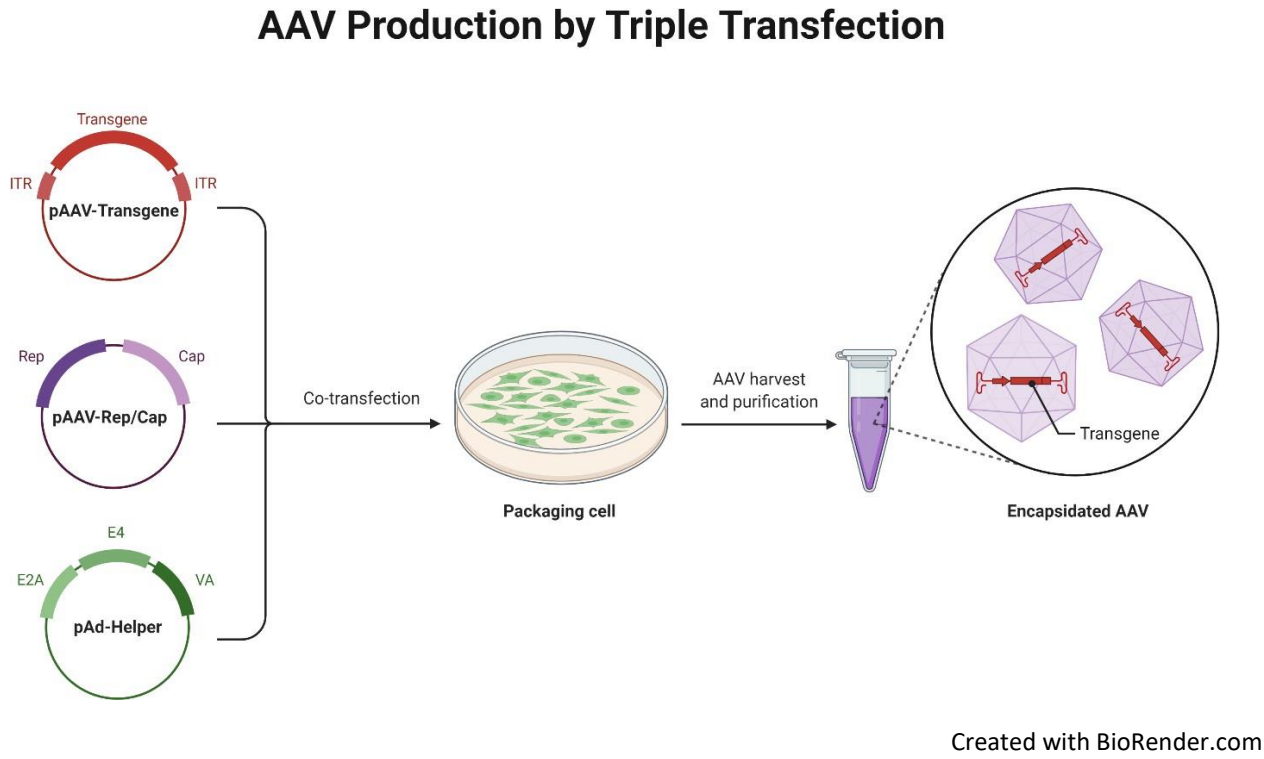

Figure 7: AAV vector Production. AAV production in HEK293 Cells involves co-transfection of triple plasmids (pAAV-Transgene, pAAV-Rep/Cap, pAd-Helper(E2A,E4,VA))

1.10 Applications of AAV Vectors in Wound Healing and Scarring

AAV vectors have already shown promise in targeting various cells and tissue in animal models. Up to date, there are over 130 clinical trials worldwide utilising the AAV technology to treat many human diseases. However, AAV based therapy for the treatment of wound healing and scarring non exist. The number of publications found in the PubMed searches using the keywords "Adeno-associated" in combination with either "skin scarring (4 hits) or wound healing" (33 hits) are very limited. Earlier studies demonstrate that AAV-mediated gene transfer into the skin has limited the *panniculus carnosus*. AAV mediated VEGF165

expression in the wound of rodents showed a significant acceleration in wound healing and a well-structured granulation and formation of new blood vessels[69], [70]. A study led by Francesco Squadrito and colleagues, using the same gene and vector in a rat burn model, demonstrated that increased vascularisation is due to the transduction of the AAVs in the skeletal muscle layer beneath the skin rodents[70]. However, the muscle layer is mainly absent in humans, suggesting that this vector may be ineffective. Another ex vivo study showed only effective transduction in Keratinocytes[71], [72]

Further investigating the AAV tropism towards dermal fibroblasts, Timothy M. Crombleholme and colleagues found that AAV5 can transduce the dermal compartment in vivo in the context of the wound[73]. However, no detailed analysis of fibroblast-specific transduction was performed in this study. Another study showed that the Intradermal injection of AAV mediated gene in porcine skin led to transgene expression limited to epidermal Keratinocytes[76]. Nevertheless, they are not successful in transducing the fibroblasts population in the porcine skin. While the results of these reports highlight the AAV tropism only confined to muscle fibers, and Keratinocytes, their clinical application is limited where the fibroblasts are the target populations in skin scarring. Until now, no study has been published investigating the AAVs as a suitable tool to target scar-forming fibroblast in the context of the wound. It is imperative to consider detailed investigations on implementing the AAV applications in wound healing to regulate the exaggerated genes in hypertrophic and keloid scars.

2. AIM OF THE THESIS

Adeno associated virus (AAV) vectors are the leading technology for manipulating gene expression to treat various human diseases. AAV is being exploited in preclinical and clinical studies for expressing cDNA and non-coding RNAs (ShRNAs, miRNAs) in tissues such as the brain, ocular, muscle, and liver. However, the utility of AAVs in skin scarring remains sparse. AAV-based targeting of the scar-forming fibroblasts population is not explored yet. The primary objective of this thesis is to evaluate the potential of AAV technology on targeting the scar-forming fibroblasts to eliminate scar severity *in vivo*. Therefore, our findings represent a significant technical advancement for scarring treatment in clinical. The specific aims of this work were to

1. Demonstrating the most effective AAV serotypes that permit efficient gene manipulation in the skin fibroblasts population.
2. Investigate the AAV based cre recombination strategy in the scar-forming fibroblasts in the context of injury.
3. Evaluating the translational efficacy of AAV mediated p120 knockdown in preventing scars in animals.

3. RESULTS

3.1 Assessment of AAV Serotype Tropism in Skin Explants

Initial experiments were designed to determine the most efficient AAV serotype for transducing skin fibroblasts *ex vivo*. Several AAV capsids (AAV2, AAV6, AAV7, AAV8, AAV9 and AAV DJ were used for packaging the AAV reporter genome that expresses eGFP driven by the human cytomegalovirus (CMV) promoter (**Figure 8**). All AAVs were incubated with murine skin-fascia explants to determine which AAV serotype could best transduce fibroblasts. Expression of eGFP in transduced cells was assessed by immunohistochemical staining using an anti-eGFP antibody three days post-infection. AAV8 displayed significantly higher fluorescence intensity when compared to other serotypes (**Figure 9A,B**). Immunofluorescent antibody staining for the fibroblast marker, fibroblast specific protein 1 (FSP1) colocalised with GFP, indicative of efficient transduction in fibroblasts (**Figure 9C**).

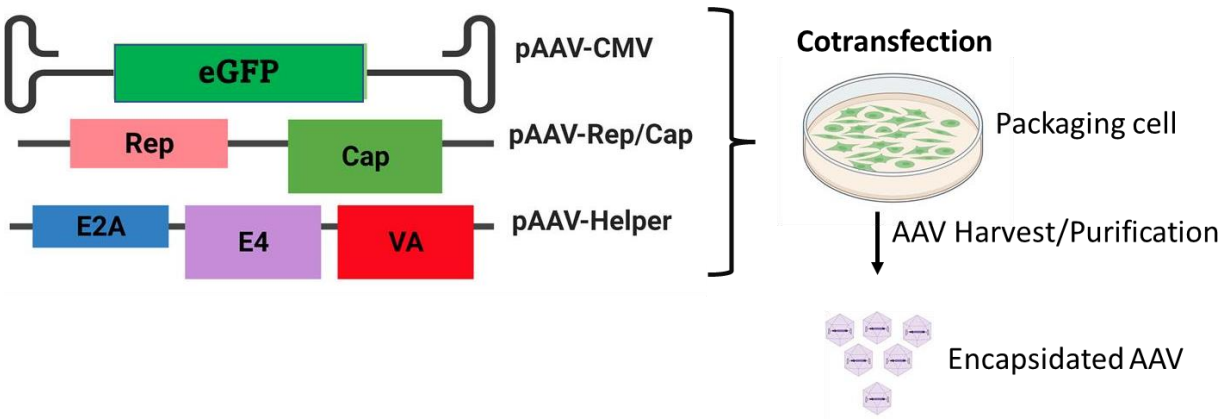

Figure 8: Scheme of AAV production using the triple plasmid transfection in AAVpro 293 T cell line.

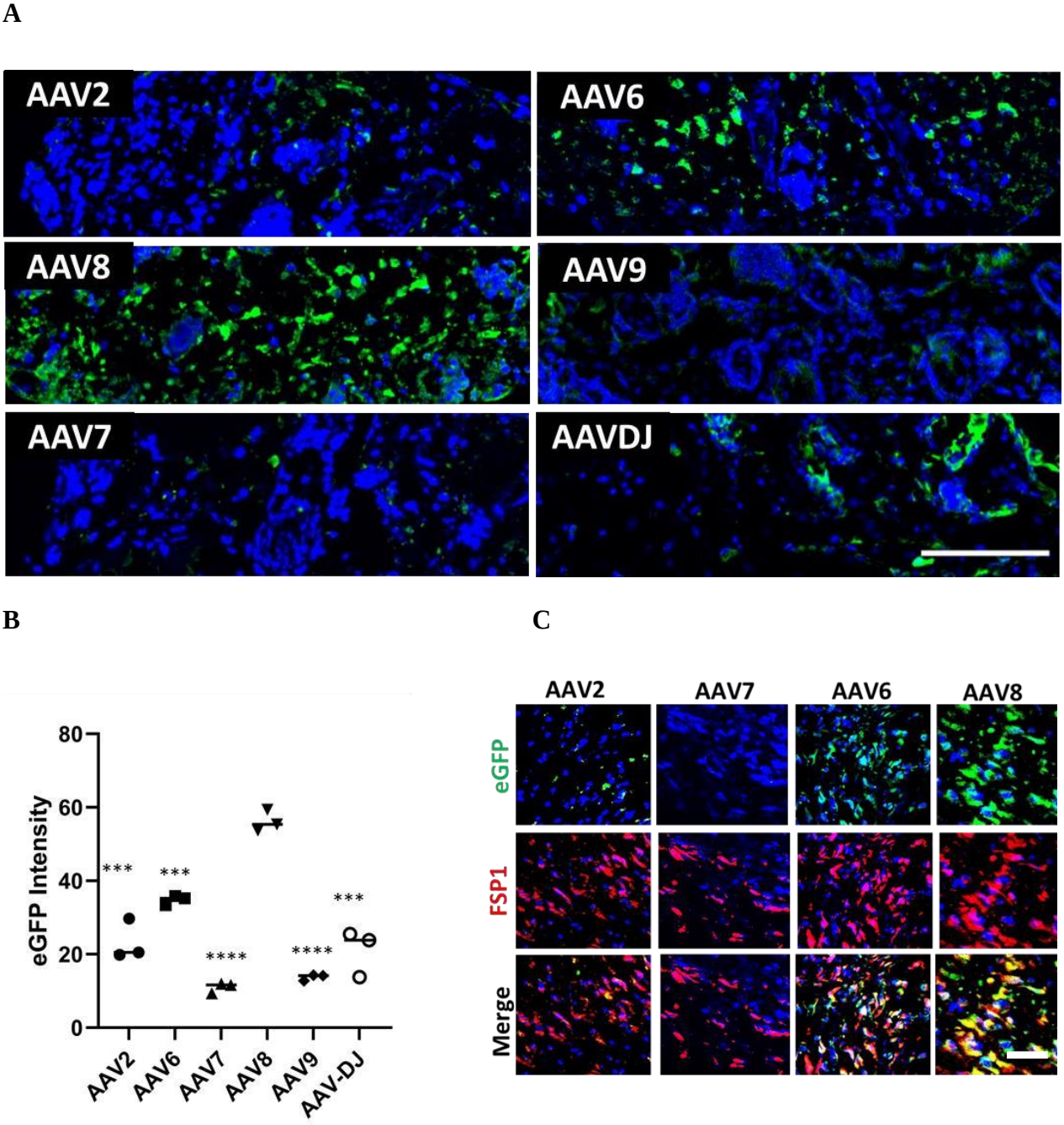

Figure 9: AAV transduces fibroblast population in the skin (A) Comparing AAV serotypes for the expression of eGFP in skin explants of C57BL/6 mice. Images show the expression for all serotypes after incubation with the AAV virus for 72 h. Green: eGFP Blue: DAPI. **(B)** Quantification of eGFP fluorescence intensity (a.u) at explant corresponding to A. Data are shown as mean ± SD. Significance tests were performed between AAV8 and other AAV serotypes. The Student's t-test calculates the p-Value. ***$p < 0.001$. $n = 3$ mice. (**C**) Confocal images of eGFP and FSP1 staining in the skin explant after transducing with different AAV serotypes. Scale bar, 100 µm.

3.2 *In vivo* Delivery of AAV8 in Fascia and Dermal fibroblasts

It is worth pointing out that AAV transduction efficiencies *ex vivo* is hardly indicative of their in vivo efficacy. Therefore, we evaluated the ability of AAV8 to transduce fibroblast populations *in vivo*. To test AAV8's ability to target the fascia *in vivo*, AAV8-eGFP was injected subcutaneously into the C57BL/6 mice at P3. The eGFP expression of AAV8 was assessed after three days post-injection. As shown in **figure 10**, we detected the CMV driven GFP expression in the fascia layer. Immunofluorescent antibody staining for fibroblast marker FSP1 colocalised with eGFP indicates efficient transduction in fibroblast cells. To address whether AAV8 can specifically transduce dermal fibroblasts, we injected AAV8-eGFP by intradermal injections. After 3 days post-injection, the collected samples showed co-immunolabeled positive for GFP and FSP1, confirming the dermal fibroblast transduction (**Figure 11)**. These results demonstrate that intradermal and subcutaneous delivery routes of AAV8 both effectively transduce dermal and fascia fibroblasts.

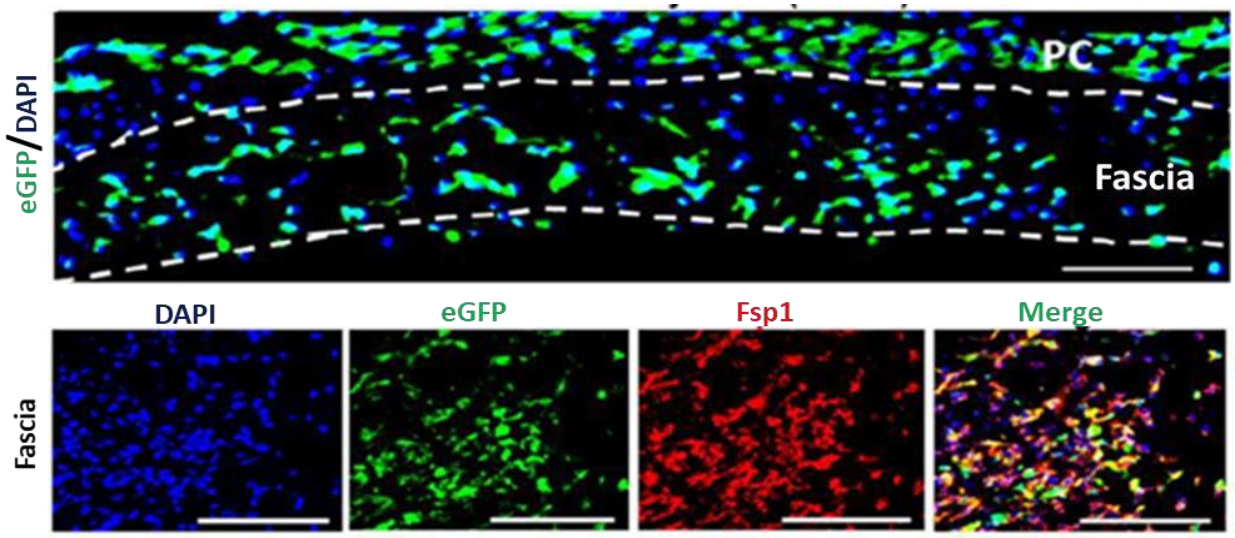

Figure 10: AAV8 infects fascia fibroblasts population in vivo. Wildtype mice were injected with the AAV8-eGFP virus into the fascia. Mice were sacrificed at 3 days post-viral injection. Immunofluorescence images eGFP-positive cells expressing mesenchymal/fibroblast marker (FSP1). Scale bar, 100 µm

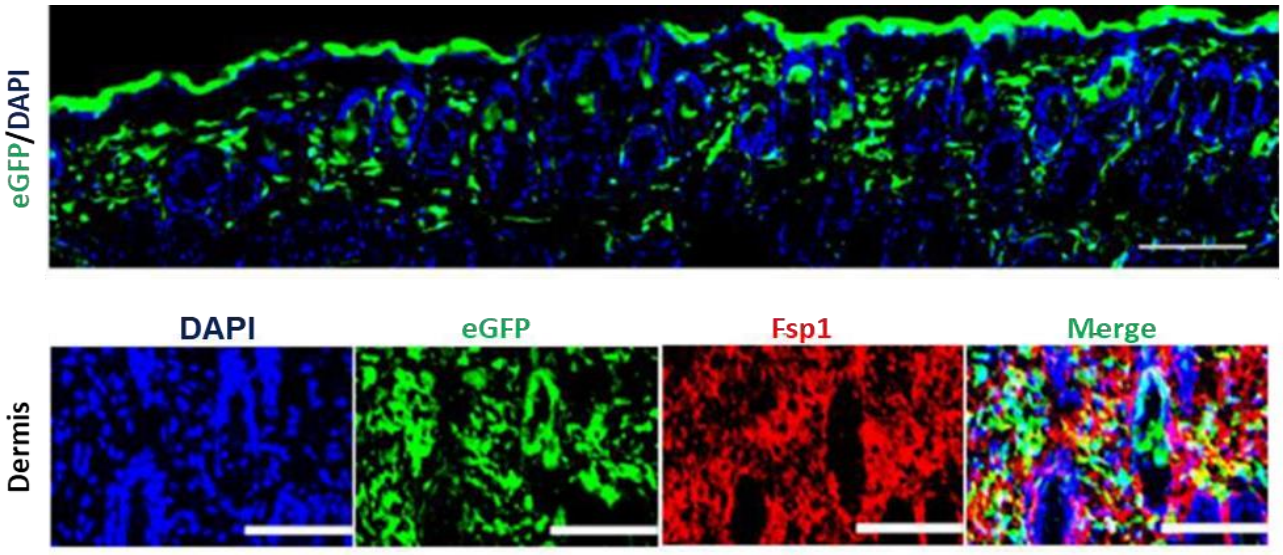

Figure 11: AAV8 infects dermal fibroblasts population in vivo. Wildtype mice were injected with the AAV8-eGFP virus into the dermis. Mice were sacrificed at 3 days post-viral injection. Immunofluorescence images of eGFP-positive cells expressing FSP1. Scale bar, 100 μm.

3.3 AAV8 Efficiently Transduces Fascia Fibroblasts

We have previously shown that fascia fibroblasts respond to skin injury by mobilising the fascia matrix into open wounds, establishing a provisional wound scar[35]–[37]. We reasoned that subcutaneous injection of AAV viral particles into the fascia region surrounding the injury site could yield efficient transduction of fibroblast cells on the wound. To evaluate whether AAV8 transduced fibroblasts steers into wounds *in vivo*, we generated the deep wound on the dorsal back skin. After the injury, we injected the AAV8-eGFP virus into the fascia layer. Seven days post wounding, about 59.4% of wound resident fibroblasts were GFP positive.

On the other hand, the uninjured fascia demonstrated 72.4% of fibroblast targeting efficiency (**Figure 12A, B**). The eGFP-positive wound fibroblasts displayed elongated and branched fibroblast morphology and stained positive for various myofibroblast markers, including ER-TR7, an antigen that is expressed in reticular fibroblasts, Dipeptidyl peptidase-4 (also known as Cluster of Differentiation 26; CD26), and alpha Smooth Muscle Actin (αSMA) (**Figure 12C, D**). Together, the method presented here allows us to target and manipulate the fascial

fibroblast cells to study the underlying mechanism of fascia associated wound healing and scarring.

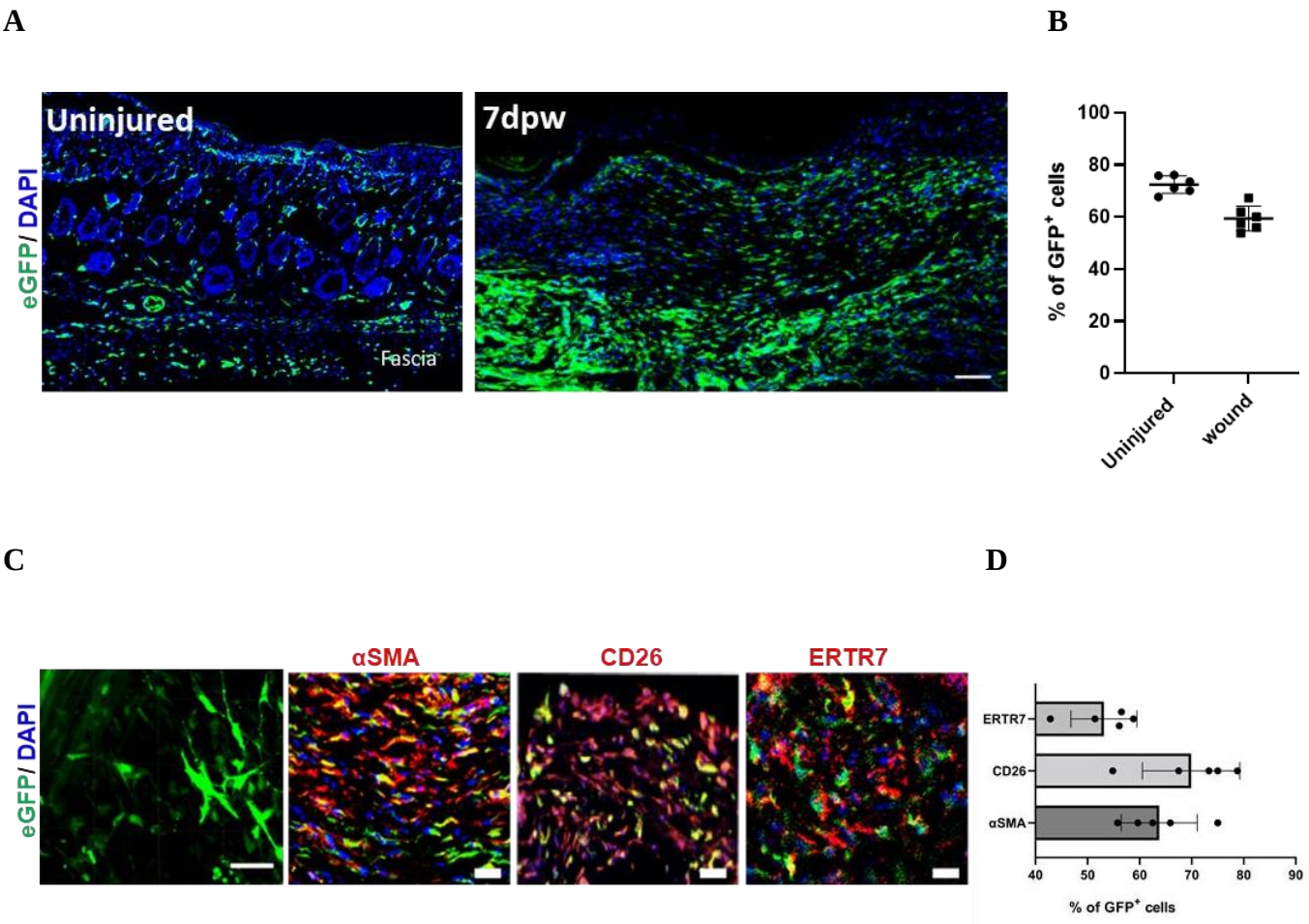

Figure 12: AAV8 injection transduce fibroblasts population in the wound. (**A**) Histology shows eGFP positive cells in uninjured skin (left) and 7dpw (right). (**B**) Percentage of eGFP cells per 100 µm corresponding to (A) Data are mean ± SD, n = 5 images analysed from 3 biological replicates. (**C**)Immunolabelling of eGFP-positive wound fibroblasts displayed elongated and branched fibroblast morphology. Immunolabelling of eGFP-positive wound resident fibroblasts from 7 days post wounding (dpw) expressing myofibroblast marker(αSMA) and fibroblast markers (CD26; ERTR7). (**D**) Percentage of eGFP cells corresponding to (C) Data are mean ± SD, n = 5 images analysed from 3 biological replicates.

3.4 AAV8 Mediated Cre Recombination in Wound Resident Fibroblasts

To specifically examine the gene modulatory prowess of fascia AAV8 transduction to steer wounds into scarless repair, we examined the efficacy of the AAV8 fascia transduction to induce efficient Cre-dependent recombination in mT/mG mice that contain a loxP-flanked STOP cassette that prevents the transcription of GFP in the absence of Cre recombinase (**Figure 11)**. AAV8-Cre induced cre/LoxP mediated recombination in mT/mG mice as resulting in expression of GFP (**Figure 12A)**. We perform the site-specific injection to determine the effect of AAV8-Cre in the dermal and fascial region in the separate mT/mG mice. We observed robust GFP signals in AAV8-Cre injected mice in dermis and fascia after 7 days injection, confirming cre-mediated recombination upon AAV8-Cre injection (**Figure 12B**).

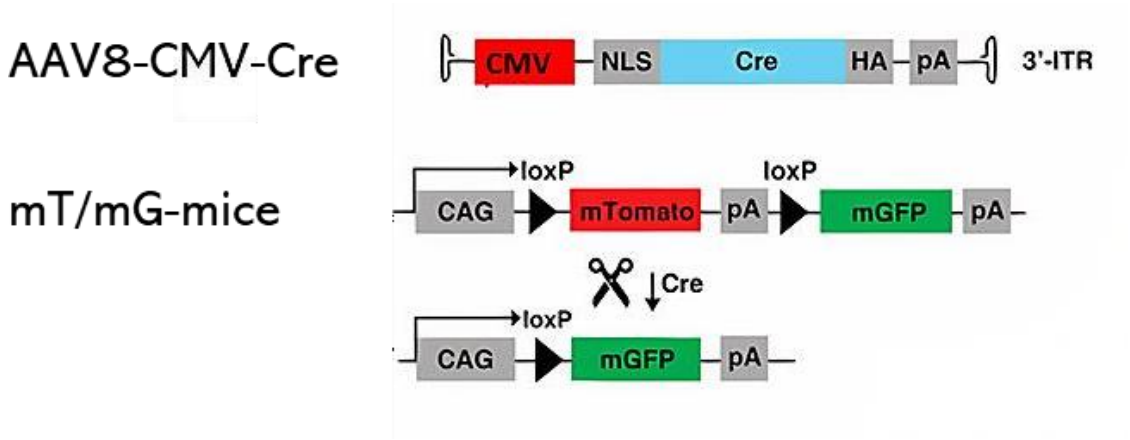

Figure 11: A, Schematic depicting the AAV8 vector-mediated Cre/Loxp recombination in the mT/mG mice allele.

A

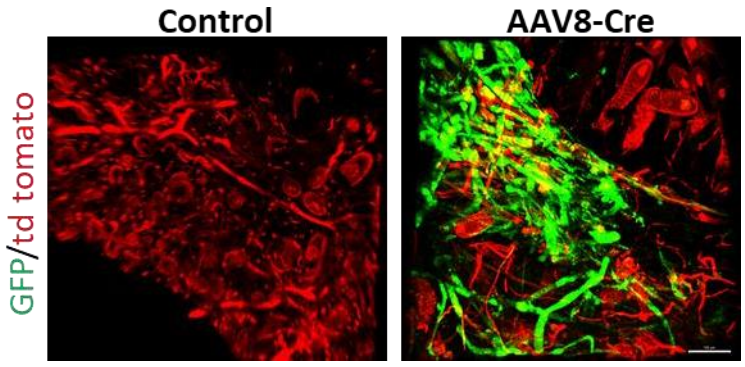

B

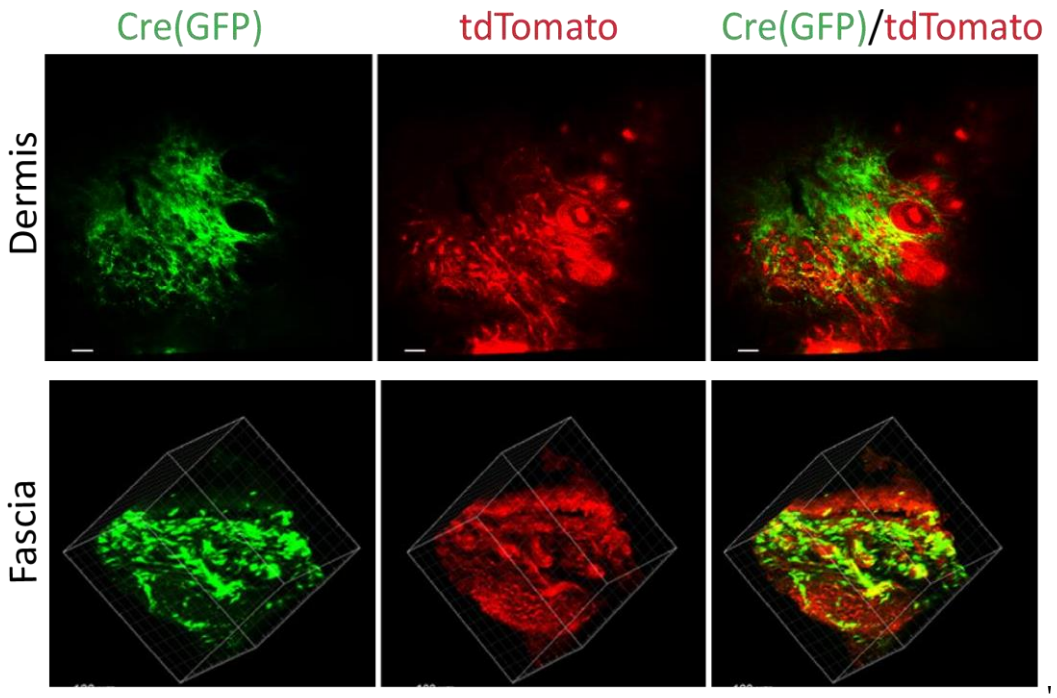

Figure 12: (**A**)Representative images of skin tissue from mT/mG mice treated with AAV8-Cre and saline (Control) (**B**) Multiphoton images of the dermis (Top) and fascia (bottom) from mT/mG mice injected with AAV8-Cre leads to constitutive expression of GFP.

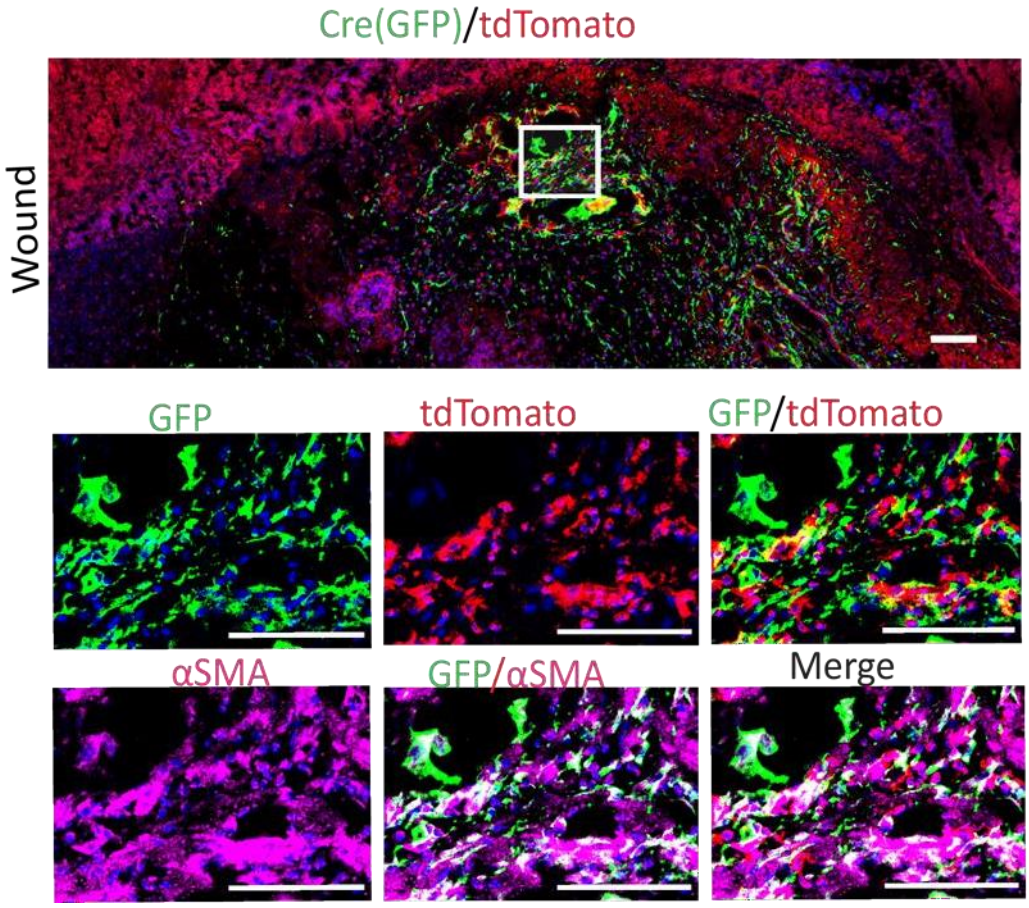

Figure 13: AAV8 Mediated Cre Recombination in Wound Resident Fibroblasts**.** Representative images of single and merged confocal images from 7 dpw show that myofibroblast marker αSMA co labelling with AAV-Cre transduced cells. Scale bar, 100 μm.

Following the demonstration of Cre mediated recombination in the uninjured mice, we then tested whether the AAV8-Cre mediated recombination system could be used to target wound resident fibroblasts in the excisional wound model. To confirm this, we generated excisional wounds on mT/mG mice and injection of the AAV8-Cre virus was performed at the vicinity of the wound. After 7 days post wounding, GFP positive cells migrated into the wound bed and colocalised with αSMA, indicating that AAV8 transduced fascia fibroblasts undergo recombination, GFP expression and migration into wounds (**Figure 13**).

3.5 p120 is an Injury-Inductive Protein in Fascia Fibroblasts

Having established a translational system for fascia modulation, we examined the gene modulatory prowess of p120-catenin (p120) to steer wounds into scarless repair. p120-catenin (p120) is an adhesion junction protein that plays a role in cell adhesion and signal transduction. Our previous studies identified N cadherin, a specific adjacent molecule essential for fascia fibroblast migration during scar formation. Furthermore, it has recently been revealed that the overexpression of N-cadherin in glioma cells relies on the expression of p120-catenin[75]. p120 also regulates N-cadherin stability through N cadherin/p120 binding[75]. Therefore, we further examined the role of p120-catenin (p120) in deep skin wounds. The results demonstrate the upregulation of p120 in injuries compared to expression levels in unwounded skin (**Figure 14A, B**). p120 had upregulated explicitly in the profibrotic lineage En1-lineage positive fibroblasts (EPFs) when deep wounds were generated En1Cre; R26mTmG mice. At 5 days post-wounding, p120 was robustly expressed and colocalised with fascia EPFs within the wound bed (**Figure 14C**). These results collectively demonstrated that p120 is highly expressed in the scar-forming fibroblast lineage throughout the wound repair process and may function in fibroblasts to regulate matrix deposition and scar formation. Therefore, we chose p120 as a candidate gene to provide proof-of-concept that systemically delivered AAV8 can direct wound severity.

A

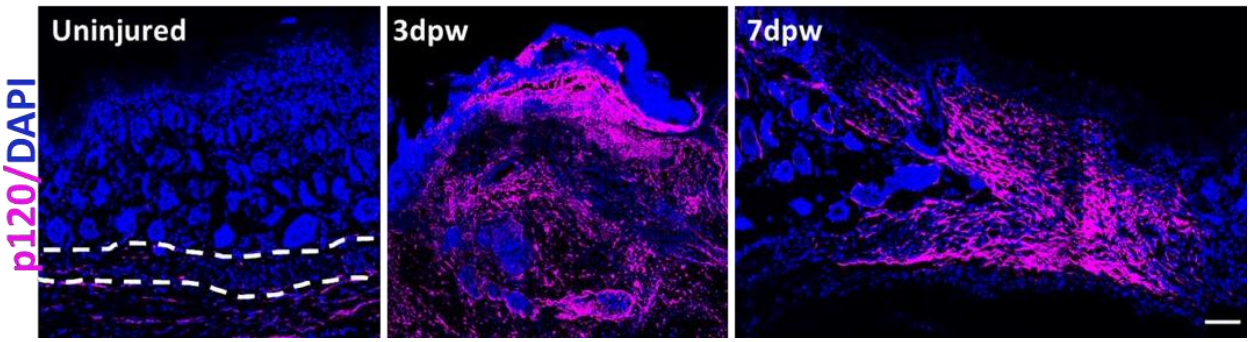

B **C**

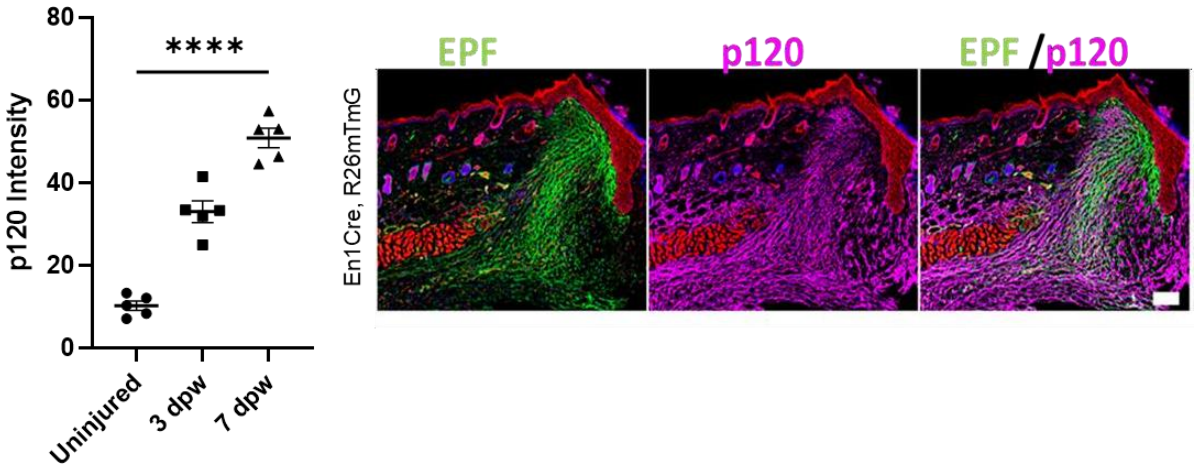

Figure 14. p120 expression is elevated in physiological wounds. (**A**) Representative confocal images of p120 expression in the uninjured fascia, 3dpw and 7dpw of C57BL/6 mice. (**B**) Quantification of P120 fluorescence intensity corresponding to A. Data are mean ± SEM, n = 5 images obtained from 3 independent experiments.The Student's t-test calculates the p-Value. ****$p < 0.0001$ (**C**) Immunolabelling of p120 expression at day 7 post wound from En1Cre, R26mTmG mice. Scale bar, 100 µm.

3.6 Validation of AAV8 Mediated Knockdown of p120 *in vitro*

To effectively knock down the p120 expression in vivo, we generated an AAV8 virus expressing either a p120 shRNA or a non-targeted shRNA (control-shRNA) from a U6 promoter and the eGFP from the human cytomegalovirus (CMV) promoter (**Figure 15A)**. To demonstrate the effectiveness of the p120-ShRNA, the primary fibroblasts were transduced with an AAV8 p120 shRNA and AAV8 Control ShRNA virus. Western blot results showed that transduction with AAV8-P120 shRNA reduced the p120 expression (**Figure 15B**). In

addition, qRT-PCR of RNA extracts from primary fibroblasts was performed to verify the knockdown specificity. AAV8-p120shRNA transduction resulted in the reduction of p120-mRNA relative to AAV Control shRNA.These data thus validated the AAV8 p120 ShRNA construct in effectively reducing the p120 expression(**Figure 15C**).

A

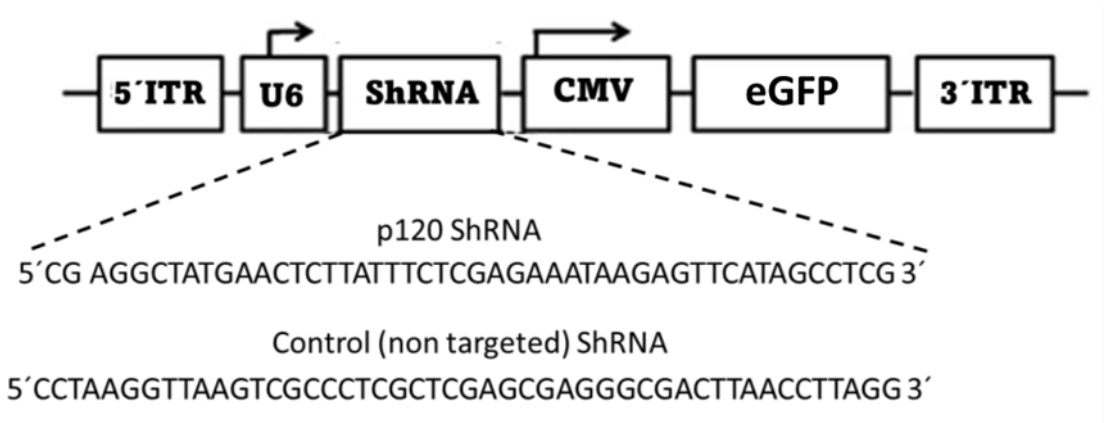

B

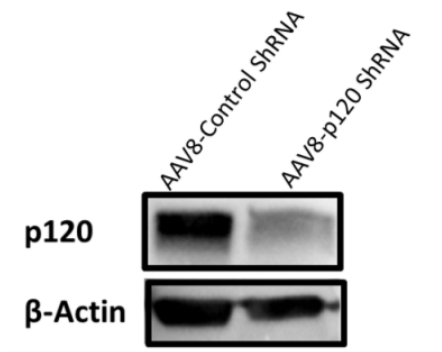

C

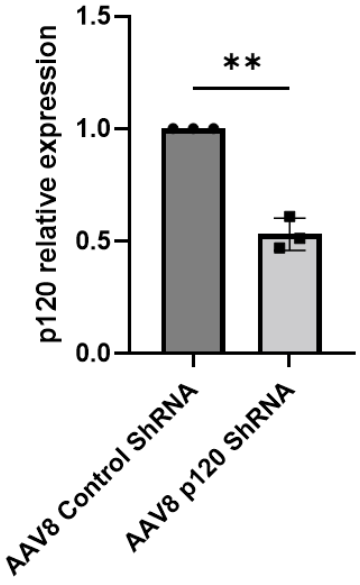

Figure 15. p120 shRNA knockdown by AAV transduction (A) Schematic representation of AAV Control ShRNA and AAV p120 ShRNA constructs. (**B)** Western blot image for Validation of p120 knockdown after AAV8 mediated p120 shRNA transduction in primary fibroblasts. **(C)** qRT-PCR analysis of p120 expression in primary fibroblasts with AAV8 expressing control ShRNA or p120 ShRNA. Data is mean ± SD; n = 3 independent experiments. The Student's t-test calculates the p-Value. **$p < 0.01$

3.7 AAV8-mediated Silencing of p120 Reduces Scarring *In Vivo*

To directly examine the relevance of injury-induced upregulation of p120 to fascia mobilisation and scar formation *in vivo*, we used AAV mediated approach to ablate the expression of p120 in fibroblasts in the context of injury. We generated the two deep wounds on the dorsal back of wild type mice. After the injury, AAV8 Control ShRNA or AAV8-p120 ShRNA virus was locally injected into the fascia layer around the wound (**Figure 16A**). After 7 days post wounding, the tissue was harvested. As shown in **Figure 16B,C**, the wound sections injected with the p120-targeted ShRNA-expressing AAV8 showed minimal p120 labelling compared to control shRNA. The total (integrated) fluorescence intensity of p120 labelling was significantly lower in the core wound expressing the p120-targeted ShRNA than control ShRNA. Myofibroblasts are the primary cell type involved in ECM deposition and engaged mainly in the progression of scarring. We further examined the effects p120 of knockdown on myofibroblast differentiation. Quantitative measurements of the immunofluorescence staining revealed a significant reduction in αSMA intensity in the wound injected with AAV8 p120shRNA compared to control shRNA (**Figure 17A,B**). Lower expression of α-SMA suggested that knockdown of p120 inhibited myofibroblast formation at the wound site. AAV8 p120 shRNA injected mice showed reduced collagen deposition in the wound than AAV8 Control ShRNA mice (**Figure 18A, B**). In addition, Scar size from AAV8 p120 ShRNA transduced was significantly smaller than those from controls (**Figure 19A,B**). Together, this study provides evidence that the p120 inhibition reduced the scar size and collagen deposition through ablating myofibroblast formation at the wound.

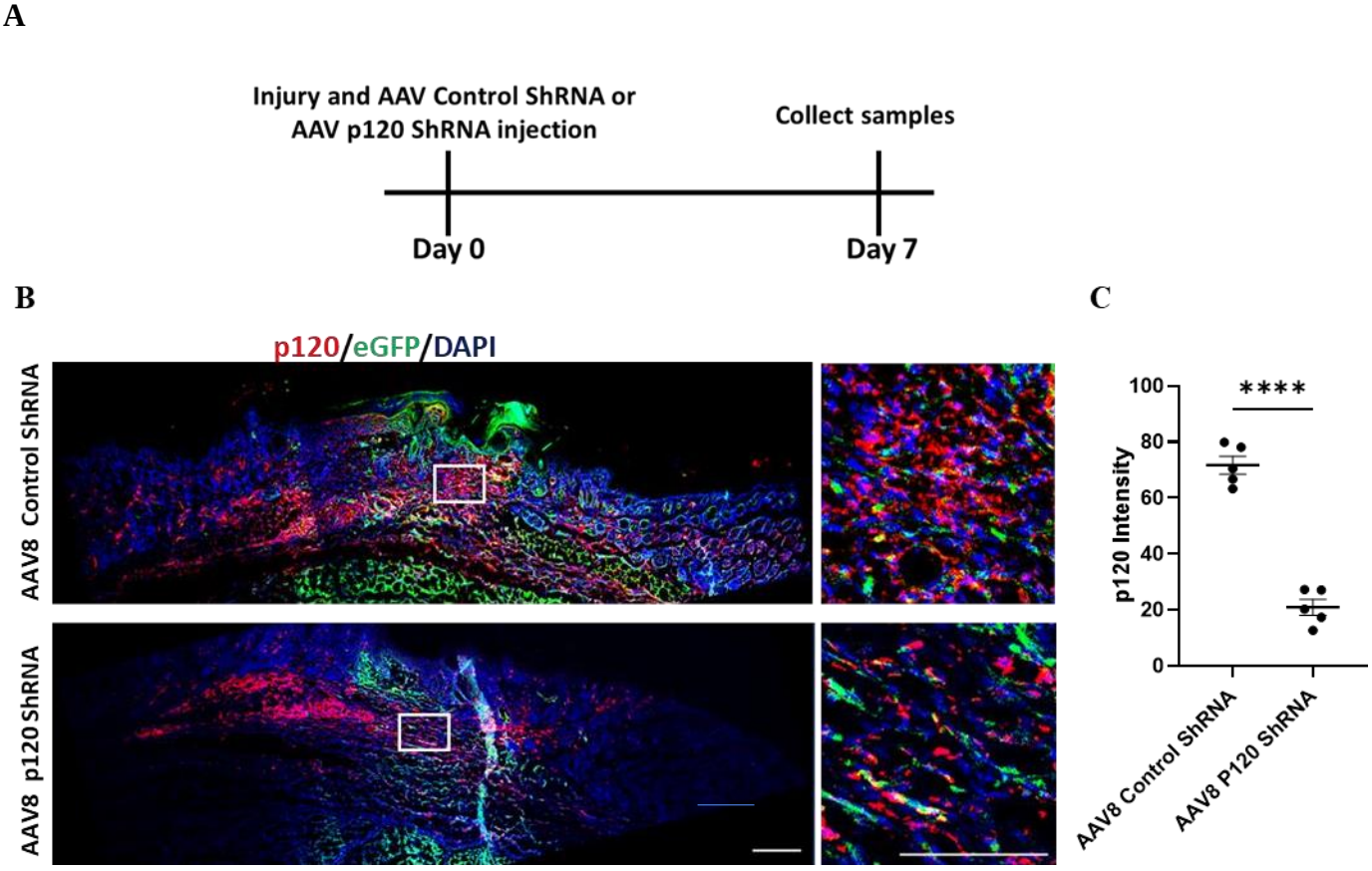

Figure 16: (**A**) Experimental scheme of injury and AAV8-p120 shRNA virus injection in C57BL/6 mice. (**B**) Representative confocal images of p120 expression in 7dpw from AAV8 Control shRNA or AAV8 p120 ShRNA injected C57BL/6 mice. (**C**) Quantification of p120 intensity corresponding to B. Data is mean ± SEM. The Student's t-test calculates the p-Value. ****p < 0.0001. n = 5.

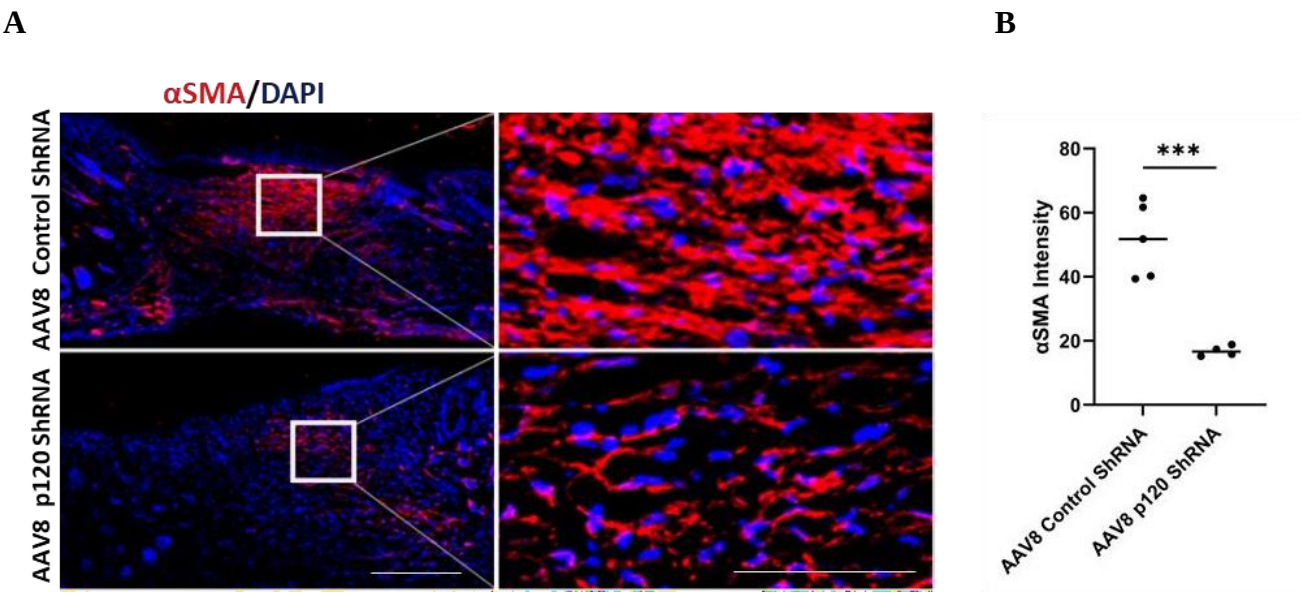

Figure 17 : (**A**) Representative images of myofibroblast marker αSMA staining in the 7dpw of AAV8-Control shRNA or AAV8 p120ShRNA injected C57BL/6 mice. (**B**) Quantification of αSMA intensity corresponding to D. Data is mean ± SEM. The Student's t-test calculates the p-Value. ***p < 0.001. n = 5.

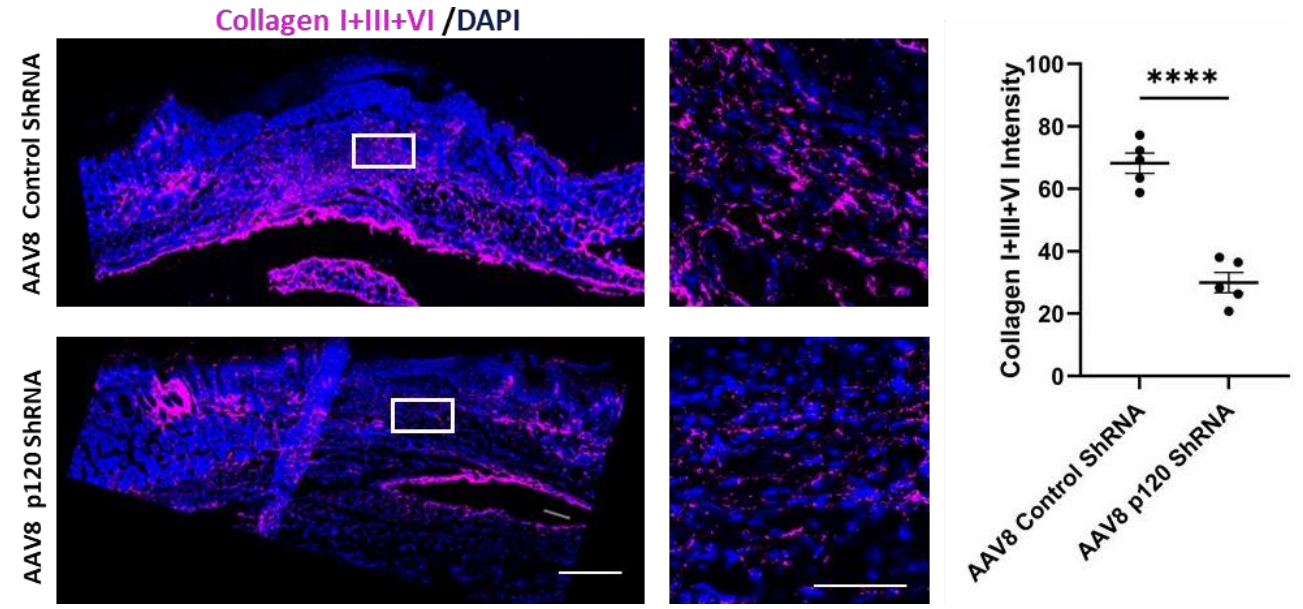

Figure 18: (**A**) Representative images of collagen I+III+IV staining in the 7dpw of AAV8 Control shRNA or AAV8 P120 ShRNA injected C57BL/6 mice. (**B**) Quantification of collagen I +III+VI intensity corresponding to F. Data is mean ± SEM. The Student's t-test calculates the p-Value. ****p < 0.001. n = 5 mice.

A B

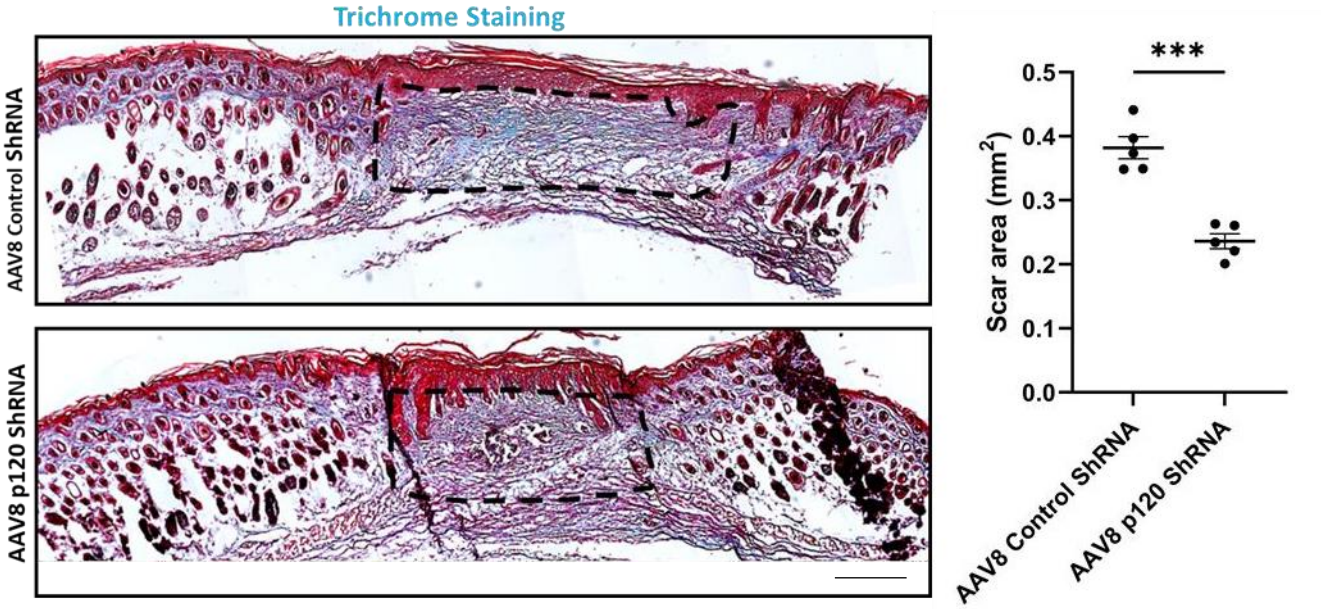

Figure 19: (A) Masson's trichrome stained 7dpw of AAV8 Control shRNA or AAV8 p120 ShRNA injected C57BL/6 mice **(B)** Quantification analysis of scar area in H. Data is mean ± SEM. The Student's t-test calculates the p-Value. ***p < 0.001. n = 5. Scale bar, 100 µm.

3.8 Fascia fibroblasts require p120 to form Protrusions and Network

Given our finding of substantial reduction in collagen deposition and scar formation upon p120 loss, we next sought to evaluate how the loss of p120 affects the scar-forming fibroblast phenotypic properties in the wound derived tissue. To further study how p120 silencing blocks fibroblast actions, we established *ex vivo* live imaging setup by directly visualising AAV transduced cells within live skin tissue. After the injury, WT mice received a subcutaneous injection of AAV p120 ShRNA or AAV Control ShRNA. After 5 days post-injection, scar tissue was excised, and live imaging was performed for 24 hrs. Control fibroblasts exhibited polarised behaviour with an extensive multicellular invasive network. Cell-cell junctions were lost in p120 silenced fibroblasts. Fibroblasts were more poorly polarised with compromised multicellular networks than the control group (**Figure 20A, B**).

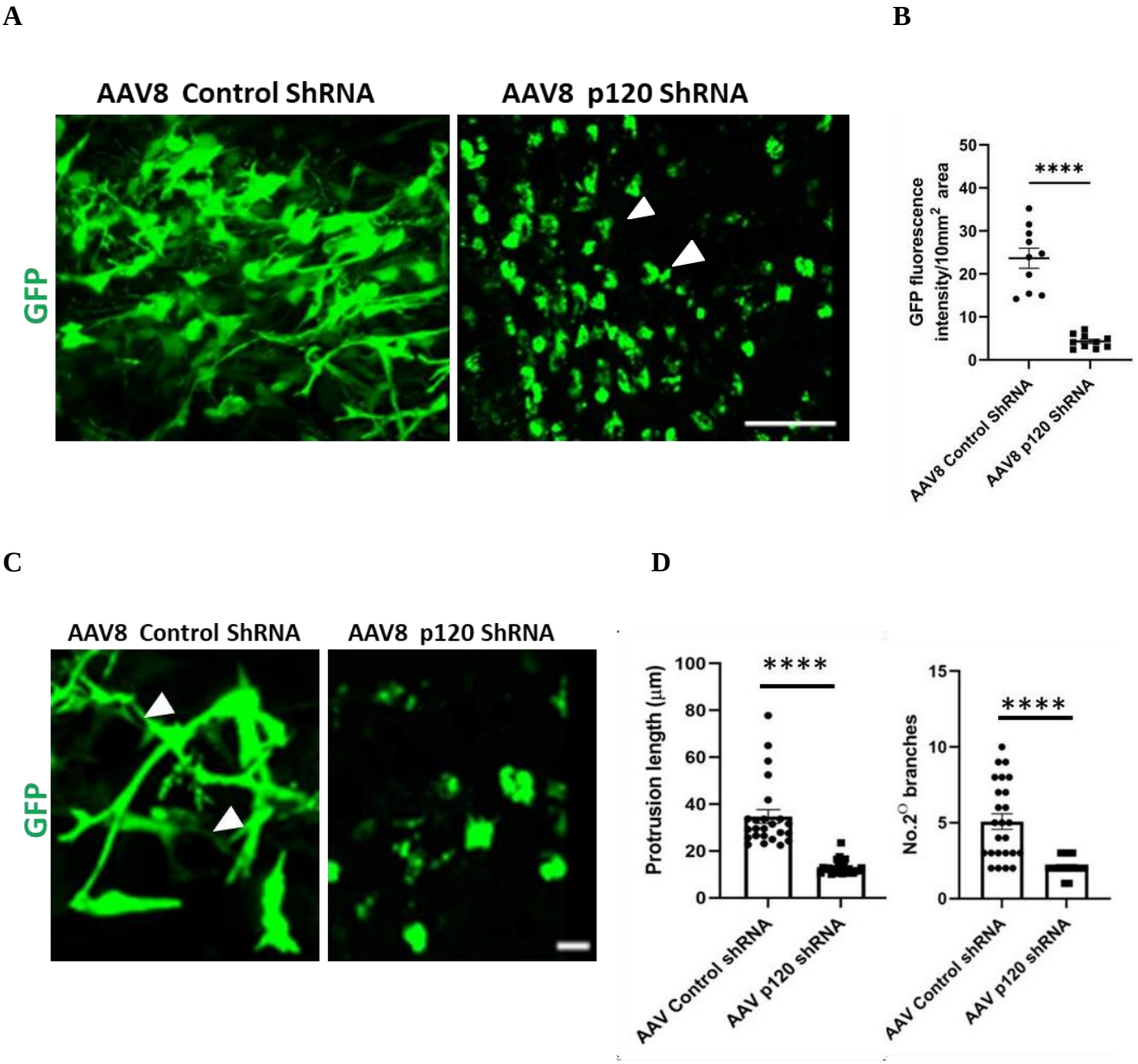

Figure 20: **Fascia fibroblasts require p120 to form Protrusions and Networks (A)** Ex vivo live images representing the morphology of wound resident fibroblasts in response to AAV Control shRNA, and AAV p120 ShRNA transduction are visualised with GFP. Arrowheads indicate individualised nonpolar cells with defective cell network **(B)** Quantification of mean GFP intensity per unit area ($10mm^2$) region corresponding to A. n = 10 sections obtained 3 biological replicates. Error bars show the SEM. ****p < 0.0001. **(C)** Impact of p120 knockdown on cell protrusion formation. Arrowheads indicate protrusion with intercellular connections. (**D**) Quantification of protrusion length and the number of filamentous branches corresponding to c. Data represent the protrusion length (µm) and the number of filamentous branching of 25 cells per condition from three independent transductions.

Further, p120 knockdown led to a significant reduction in fibroblast protrusion length and branching compared to control fibroblasts (**Figure 20C,D**). In addition, particle image velocimetry (PIV) analysis demonstrated that control EPFs exhibit directed movement with collective migration within the wound region, whereas p120 silenced cells lose this collective migration behaviour (**Figure 21**). These results indicate a crucial role of p120 in acquiring protrusion formation and stabilising filamentous cell-cell interactions needed for effective collective migrations of scar-forming fibroblasts into the wound.

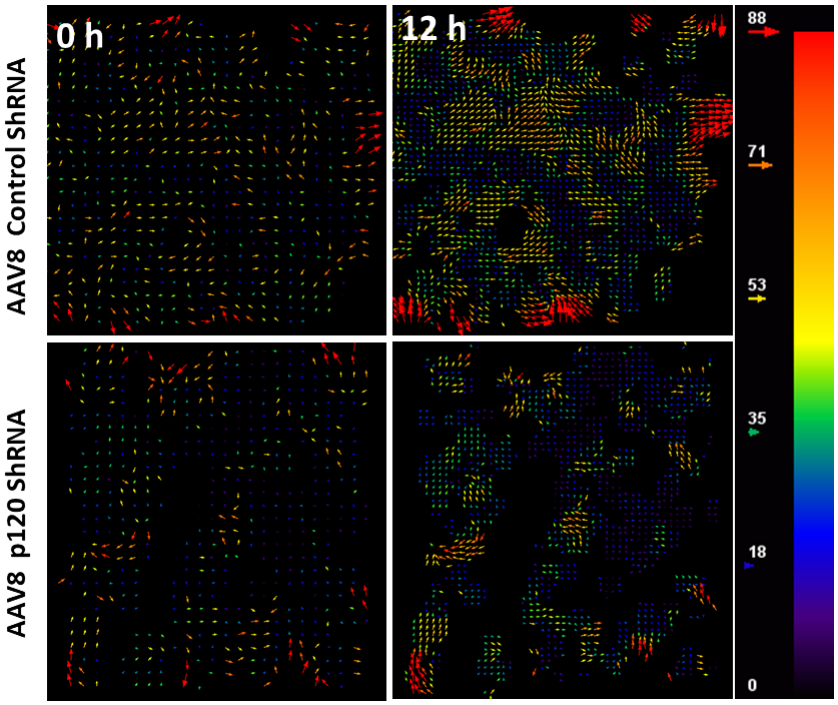

Figure 21: Particle image velocimetry (PIV) analysis perform GFP expressing cells from to cell movement pattern in response to AAV8 Control ShRNA and AAV8 p120 ShRNA transduction at indicated time points. The arrow colour indicates the different speeds corresponding to the scale bar. Slow (blue) to fast (red). Scale bar unit: pixel. The data are extracted from the supplementary video 1 and Video 2

3.9 p120 Knockdown Inhibits Fascia ECM Movements into Wounds

Recently we showed that fascia resident EPF fibroblasts physically mobilise the fascia ECM into the wound[35]–[37]. To further investigate whether p120 depletion in fibroblasts blocks mobilisation of fascial ECM *in vivo*, we fluorescently 'labelled' the fascia ECM with NHS-ester to conjugate the amine residue prior to the wound (**Figure 22A**). 3mm deep wound (removing, i.e., epidermis, dermis, and fascia) on the back skin using a biopsy punch. After the injury, AAV8 Control or AAV8 p120 ShRNA was subcutaneously injected around the wound edge. At 7 days post-wounding, AAV8 control ShRNA-injected wounds showed that 64.8% of the wound bed matrix had NHS ester labelling that moved from the adjacent fascia.

In contrast, only 28.9% of labelled fascia matrix contributed to AAV8 p120 ShRNA injected wounds (**Figure 22B,C**). Collectively, our in vivo experiments demonstrate that p120 is highly increased in fascia fibroblast after injury. It facilitates their migration, which is required for the ECM mobilization from the fascia into wounds to plug the wounds and establize the scars. Furthermore, AAV p120 shRNA efficiently modulates fascia mobilization, producing scarless skin wound healing.

A

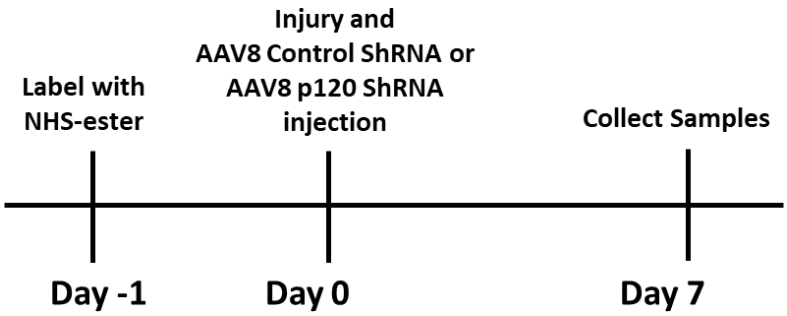

B **C**

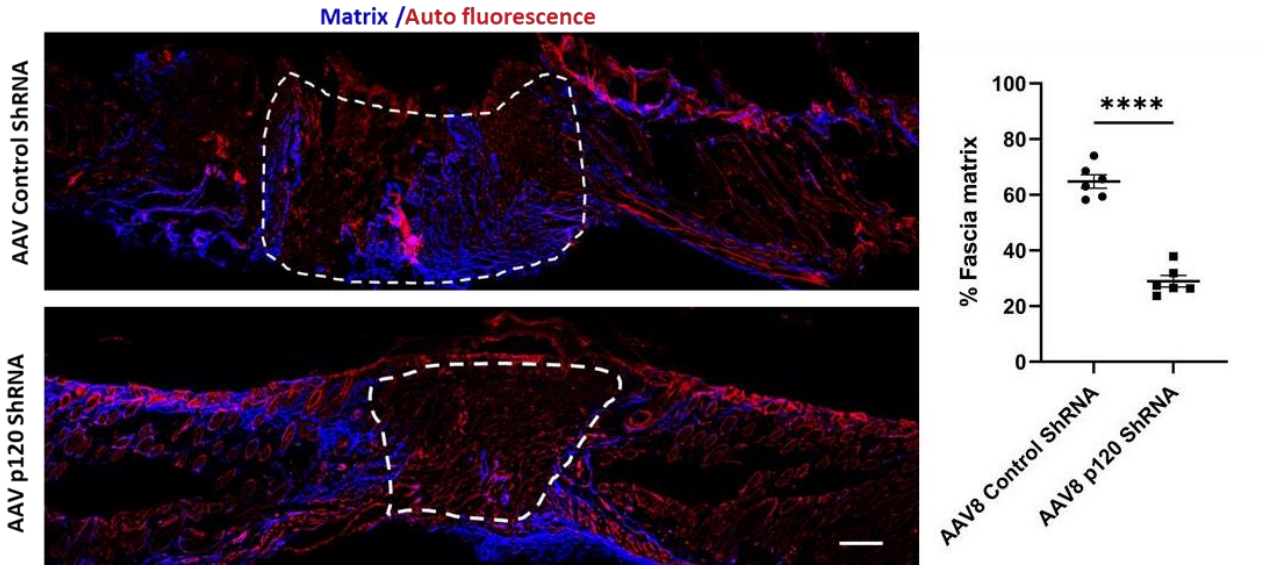

Figure 22: **(A)** Experimental scheme of matrix labelling with AAV Control ShRNA or AAV p120 ShRNA injection after injury in C57BL/6 mice. **(B)** Images show NHS ester labelled matrix in 7dpw. Labeled fascia matrix in blue and autofluorescence in red **(C)** Percentage of labelled fascia matrix coverage in B. Data is Mean ± SEM, n = 6 sections from 3 independent experiments. unpaired two-tail Student's t-test, ****p<0.001.

4. DISCUSSION

Current clinical practice of dermal scar tissue relies on scar tissue management rather than therapeutic amelioration, including diverse topical management options that are either non-invasive or invasive treatments[30]. Current invasive treatments include surgical scar corrections, intralesional application of corticosteroids, and physical laser- or radiotherapy, some of them in combination, e.g., radiotherapy directly after surgical scar correction[40]. Non-invasive treatments of visible scar tissue include applying pressure forces, often in combination with applied silicone sheets and gels[42]. In addition to these applications, many non-evident treatment options are offered, including dermatologic ointments, oils, lotions and creams, and physical measures such as static and dynamic splints and massage therapy [43], [48], [76]–[79]. A provisional wound scar is formed when the subcutaneous fascia resident fibroblasts physically mobilise into wounds due to deep skin injuries[35]. Therefore, the fascia fibroblast around the wound region should be the primary target of therapeutic interventions. In vivo fascia modulation is hindered by a lack of efficacious approaches for targeted modulation of fascia tissue in vivo and a translational gap in our understanding of scar mechanisms. There has been no efficient demonstration of targeting the sources of scars from the fascia for scarless wound repair. Here, we overcome these two milestone gaps by establishing an AAV method that recombinant AAV8 serotype targets fascia fibroblasts and allows gene manipulation of fibroblasts in the context of injury. Replication-deficient AAV is normally endocytosed and taken to the nucleus by the association of its capsid proteins with surface receptors of host cells [97], [98].AAV vectors are safe and effective in various preclinical and clinical studies. The success of AAV as a gene delivery platform is due to many characteristics, including its long-term transduction efficiency, lack of pathogenicity, and relatively low immunogenicity [82].

Moreover, AAV vectors can persist in post-mitotic cells of host tissues for years. A nonviral

vector, on the other hand, such as nanoparticles or liposomes, can degrade rapidly, can be cleared in the circulation, is biologically short-lived and generally does not exhibit specific uptake. The transduction mechanism underlying the tropism of the AAV8 vector in fibroblasts remains unknown. A critical step in viral entry into the fibroblasts is the recognition of specific cell surface membrane glycoproteins as receptors.

Interestingly AAV8 was also found to mediate the eGFP expression within the scar area when you transduce fascia cells after injury. This represents an additional advantage for manipulating the potential therapeutic genes in the scar-forming fibroblasts that migrate to the area of injury. The AAV8 Cre infection resulted in GFP recombination of loxP-flanked genes in the dermis and fascia. Additionally, the results demonstrate that AAV8 Cre can cause recombination in the myofibroblasts population within the wound bed. The delivery of AAV Cre to scar-forming fibroblasts represents a valuable approach to turning various genes' expression ON or OFF. In short, AAV8 Cre mediated recombination eliminates the need for time-consuming and costly breeding techniques and eliminates complex breeding approaches with genetic backgrounds where gene deletion causes embryonic lethality. It facilitates direct comparison of littermates homozygous for a loxP-flanked allele with different sides of the dorsal back skin of the same animal after viral injection. Moreover, AAV8 Cre in the combination of iDTR mice will be a powerful tool for the ablation of fibroblasts to test their role in scarring and wound healing.

Another milestone of this study is identifying p120 as a targetable molecule for scar prevention that is selectively expressed in fascia fibroblasts in response to injury. p120 catenin regulates cell-cell adhesion by playing a critical role in regulating cadherins' stability [102]. p120 has an essential role in the invasion and migration of glioma cells. High expression of p120 has been shown to enhance the motility of cultured fibroblasts [84]. However, the physiologic relevance of p120 in modulating fascia steering and skin wound

repair has not been demonstrated. Our study discovered the physiologic role of p120 in maintaining a supra-cellular organisation of fascia fibroblasts needed for fascia steering. Importantly, our results showed that AAV8 mediated silencing of p120 modulates the extent of connective tissue steered into wounds, reducing matrix deposition and scar severity in wounds.

In conclusion, our findings open a wide range of possibilities for future work exploring the therapeutic effects of AAV-mediated gene therapy used in the context of wound healing and scarring. Although AAV8 vectors target scar-forming fibroblasts with high efficiency, they also tend to transduce other types of cells in the skin. Future studies will focus on identifying the unique fibroblasts markers and incorporating the fibroblasts specific promoter in the AAV constructs to overcome this challenge. Therefore, it is anticipated that future improvements in the AAV vector design, such as the use of scar-forming fibroblasts-specific promoters in AAV vector genome design, or even further improvement in capsid design, will allow even more specific delivery of therapeutic genes without causing any nonspecific transduction. Because of the ubiquity of scar development across organs, diseases, and pathologies, such an AAV mediated anti-scar therapy may have broad clinical implications and pharmaceutical value.

5 MATERIALS AND METHODS

5.1 Antibodies

The following antibodies were used: anti-goat FSP1 (1:200, ab58597), anti-mousep120 catenin (1:250, BD610133), anti-rabbit αSMA (1:250, ab5694), anti-rabbit Collagen type I (1:250, Rockland 600-401-103-0.1), anti-rabbit Collagen type III (1:200,ab7778), anti-goat CD26 (1:200,SAB2500328), anti-rabbit collagen type VI (1:200,ab6588,1:150), anti-rat ER-TR7 (1:500,ab51824), anti-rabbit GFP (1:250,ab290).Tissue sections were over layed with relevant secondary antibodies (1:500) for 1 hour at Room Temperature (RT).

5.2 Tissue Fixation and Cryosections

The skin tissue was fixed with 2% paraformaldehyde (PFA) at 4 °C for overnight. Following removal of PFA, samples were rinsed in PBS three times for a total of 5 minutes each. Immerse tissue in 30% sucrose overnight. Embed the tissue in Tissue-Tek® O.C.T medium and placed at -80 °C. The tissue block was sectioned at 10µm thickness in the cryostat (Cryostat NX70). Tissue mounted on Fisherbrand SuperFrost/Plus slides. Slide boxes were stored at -70° C until ready for staining.

5.3 Immunofluorescence Staining

Cryosections were fixed with ice-cold acetone for 5 minutes, gently wash the slides 3X in PBS. Overlay the tissue section with a blocking solution. Incubate the slides in a humidified chamber at RT for 1 hr. After that, slices overlayed with a primary antibody with recommended dilution in blocking solution overnight at 4°C. The next day, gently wash the slides 3X in PBS (5 min/wash). Overlay the tissue sections with secondary antibody diluted in blocking solution. Incubate the slides in a humidified chamber for 1 hr at room temperature. Gently

wash the slides 3X in PBS (5 min/wash) and stain with DAPI solution (1:5000 dilution in PBS) for 5 min. Gently blot the slide with absorbent paper to remove excess liquid. Fluoromount-G™ Mounting Medium(Invitrogen) was used for Mounting the slides. The mounted slides were imaged using a confocal laser scanning microscope (Zeiss LSM710).

5.4 Masson's Trichrome Staining

Fix the slides by immersion in precooled cold acetone (-20°C) for 5 min. Incubate the tissue slides with Bouin's solution (Sigma-Aldrich HT10132) at RT overnight. After washing the slides for 2 minutes with cold tap water, they are stained for 10 minutes with iron Hematoxylin solution (Sigma-Aldrich HT1079). Discard the Hematoxylin solution. Wash the slides with running tap water for 10 minutes. Following that, rinse the slides with distilled water for 2 minutes. Incubate the Slides for 5 minutes with Biebrich Scarlet-Acid solution. Wash the slides with 3X distilled water (1min/wash). Incubate the slides with Phosphotungstic/Phosphomolybdic Acid Solution for 10 minutes in the glass chamber and directly incubate the slides with Aniline Blue solution for 10 minutes. Wash the slides with 3X distilled water for 1 minute each. Further, incubate the slides with Glacial acetic acid (1%) for 2 minutes and wash the slides with 2X distilled water for 1 minute each. Post staining, the tissue slides were dehydrated with 70% ethanol for 3 minutes - 90% ethanol for 3 minutes and 100% ethanol for 3 minutes. Finally, keep the slides in Xylol for 5 minutes. After dehydration, the slides were mounted with 2-3 drops of ROTI®Mount media. Images were acquired using the Zeis Axio imager with 20X magnification. The stained structure in the slides represents the following, Nuclei- Black, Cytoplasm-Red and Collagen in Blue.

5.5 Cell Culture

AAVpro293T cell line (Takara Bio, cat. no. 632273) and primary fibroblasts were cultured in DMEM containing 10 % FCS (Fetal Calf Serum), 1%GlutaMAX™, and 1% Penicillin-Streptomycin (PS). The cells were all grown under the conditions of 37°C, CO2 at 5%, and 95 % relative humidity in an incubator. Gently wash the cells with PBS and overlay with trypsin-EDTA. Following the addition pre-warmed complete growth medium, cells were centrifugated at 200 x g for 5minutes. Dilute the cell suspension and seed into the new flask with the recommended cell density and return the cell flask to the 37°C incubators.

5.6 Isolation of Primary fibroblasts from Mouse

Primary skin fibroblasts were obtained from neonatal (P0-P4) back skin tissue. Mince the tissue with scalpels in a 10cm dish and transfer the tissue fragments into a centrifuge tube containing collagenase (1000U/mL) final concentration. Incubate the tube at 37°C for 30 minutes and swirl the tubes every 5 minutes. Centrifuge at 200 x g for 10 min. Remove the supernatant and resuspend the pellet with 2 ml of HBSS medium. Centrifuge the cell suspension again at 200 × g for 5 minutes and 0.5ml of 0.05 % trypsin, swirl the tube vigorously and place the tube for 30 min at 37°C. Then centrifuge the cell suspension at 200 × g for 5 minutes and discard the resuspend. Resuspend the cell pellet with 2 ml of fibroblast culture medium. The cells suspension was filtered with a 70µm cell strainer. Transfer the cells to a 10 cm cell culture dish and 10 ml of culture medium. Incubate the cells at 37°C, CO2 at 5%, and 95 % relative humidity in an incubator.

5.7 AAV Production and Purification

AAVpro 293 T cell line (Takara Bio, cat. no. 632273) were cultured in a 15 cm tissue culture (20 dishes in total). The cells should reach the confluence of 75%-80% on the day of

transfection. Prepare a 1:1:1 molar ratio of triple plasmids (pRC6, helper plasmids and AAV transgene plasmids). We used the link (https://nebiocalculator.neb.com/#!/dsdnaamt) to calculate the DNA amount for transfection. The total DNA is calculated based on 0.5µg of DNA/cm^2 of cell culture surface area. The volume of Polyethyleneimine (PEI) was used based on 4:1 ratio of PEI (ug): total DNA (ug). 4 days after transfection, scraping off the cells with a rubber policeman, centrifuged at 1700g and RT for 10 min. The cell pellet was used to extract the AAV virus according to the AAVpro® Purification Kit (Takara. Cat. #6232) procedures. Resuspend the cell pellet with AAV Extraction Solution A at RT for 5 min and centrifuge at 9,000g for 10 min. Collect the supernatant and 1/10 volume of AAV Extraction Solution B. 1/100 volume of Cryonase Cold-active Nuclease was added to the viral suspension and incubated for 1 hr at 37°C water bath. Following that, 1/10 volume of precipitator A was added to the solution, vortexed for 10 seconds and incubated for 1 hr at 37°C water bath. An additional 1/20 volume of Precipitator B was added and then centrifuged at 9,000g for 5 minutes at 4°C. Following that, a Millex-HV 0.45µm filter was used to filter the supernatant out of the solution. AAV containing filtrate was transferred into an Amicon Ultra-15,100 kDa filter device. The filter was centrifuged for 5 minutes, at 2,000g, at 15°C. The centrifuge was continued until the total volume of AAV containing filtrate was less than 400µl. Discard the filtrate and resuspend the AAV containing solution by pipetting. The vector particles were aliquoted and stored at –80 °C for the long term.

5.8 Viral Titer Measurement by qPCR

AAVpro® Titration Kit was utilised to measure the genomic titer of AAV stock. The AAV sample was treated with DNase I and incubated at 37℃ for 15 minutes to digest the producer cells' encapsidated and free DNA. To inactivate the DNase I, the AAV samples was incubated at 95℃ for 10 minutes. AAV samples were lysed by adding the equal lysis buffer volume and

incubating at 70℃ for 10 minutes. The viral sample has been diluted at 1/50 using EASY Dilution and use the diluted AAV sample as a template for qPCR. Each sample was set up an of 20µl as a reaction volume: 5 µl of AAV sample or standard DNA is added to the 12.5µl of SYBR master mix,0.5ul of primer mix (forward and reverse 10µM each), 1µl of Universal Probe Library and 1µl of nuclease for the reaction. The qPCR samples are run as triplicates in 96-well plates using the Roche LightCycler 480 II system. PCR conditions were 2 min at 95°C, followed by 35 cycles of two steps profiles consisting of 95°C for 5sec and 60°C for 30Sec. Plot Ct value (Y-axis, linear scale) vs Virus titer (X-axis, logarithmic scale) Generate a standard curve using the Ct and the titre value of 6 standard Control DNA dilutions. The titre value of the unknown virus sample was calculated using y = mx + b from the trendline equation. The R2 value should be > 0.95. The dilution factor was taken into consideration for the final titer calculation.

5.9 Western Blot

Cells were directly lysed using RIPA buffer (Sigma-Aldrich, UK) supplemented with a phosphatase inhibitor cocktail (Protease Inhibitor Cocktail Set III, EDTA-Free, Calbiochem, UK (1:200 dilution). With the BSA protein assay kit, the protein concentration was determined. All assays were performed using a total of 30µg of protein. Using a thermo-block, all proteins were denatured at 100°C for 5 minutes. All samples were kept on ice until they were used after denatured. Proteins were separated on Invitrogen™ NuPAGE™ 4 to 2% Mini gels using an electrophoresis technique described by the manufacturer (running conditions 200V and 135 mA). Proteins were blotted onto polyvinylidene difluoride membranes (PVDF) from polyacrylamide gels. The blocking step was performed for 1 hr in 5% skim milk in TBST (Tris-Buffered Saline Tween-20). After blocking, membranes were kept with specific anti-p120 antibodies overnight at 4°C (antibody dilutions were prepared in blocking buffer). Two

washing steps were performed using 0.1% Tween (in PBS) for 10 minutes each. Secondary antibody dilutions were prepared in blocking buffer then incubated for 1 hr at room temperature on gentle shaking. The PVDF protein membranes were developed using an ECL™ detection kit. p120 protein bands were visualised using a chemiluminescent imaging system such as a ChemiDoc in a dark room. β-actin was used as a loading control.

5.10 RNA extraction from Primary Fibroblasts

We used Qiagen RNeasy Mini-Kit to extract the RNA from primary fibroblasts. RNase-free water and RNase-free reaction tubes were used to avoid any possible RNase activity during the procedure. A total of 350µl of RLT buffer was employed for every $5x10^6$ cell. The samples were incubated at RT for 5 minutes. Add 350µl of 70% ethanol was added into the cell lysate. A total 700µl volume of lysed sample was transferred into the RNeasy spin column, placed into the collection tube and centrifuged for 60 sec at 14000 rpm. After discarding the flow-through, 600µl of RW1 buffer was added to the column and centrifuged for 60 sec at 14000rpm. After removing the flow-through, the spin column was placed in a new collector tube, and a 500µl RPE buffer was added. The column was centrifuged for 60 sec at 14000 rpm, and the flow-through was discarded. The columns were transferred into a new Eppendorf tube, and 35µl of Nuclease free water was added into the spin column membrane and centrifuged for 60 sec at 14000rpm to elute the RNA. RNA samples were quantified using a Nanodrop ND-1000.

5.11 cDNA Synthesis

Verso Reverse Transcriptase (Invitrogen) was utilised for cDNA synthesis. Briefly, 5µl of RNA template was added in 4µl of cDNA synthesis buffer, 2µl dNTP mix, 1µl RNA primer,1µl RT enhancer, 1µl Verso Enzyme mix, in a total volume of 20µl cDNA synthesis reaction.

The reaction tubes were incubated at 42°C for 30 minutes and 95°C for 2 minutes.

5.12 qPCR

The following quantitative reverse transcription-PCR procedures were carried out in a final reaction volume of 10µl using a LightCycler® 480 II platform (Roche Diagnostics): 4 µl of cDNA is added to the 5µl of Light Cycler® 480 probes master mix (Roche Diagnostics), primer mix (forward and reverse 10µM each), 1µl of Universal Probe Library (Roche Diagnostics) and 0.7µl of nuclease for the reaction. The qPCR samples are run as triplicates in 96-well plates using the LightCycler 480 II device (Roche). The PCR profile condition was at 95°C for 5min, 45 cycles of denaturation at 95°C for 10sec, and 60°C for 30Sec. Finally, a cooling phase of 30 sec at 40°C was carried out. The gene expression levels were normalised to the internal reference gene RPL-13A. Data are analysed by the $2^{-\Delta\Delta C_T}$ method.

Forward Primer : 5´ CTGTGATGGTGTTCCTGCTCTG 3´
Reverse Primer : 5´ TGGGATGAGAGATTCCACAGGG 3´

5.13 Animals

Wild type (C57BL/6J, En1^{cre}, *R26^{mTmG}*) mouse were purchased from Jackson Laboratories or obtained from Stanford University Research Animal Facility. The mouse lines were kept at the Helmholtz Animal Facility. The mouse was maintained in a controlled environment witha light-dark cycle (12h light and 12h darkness). Animals were housed in clean and ventilated cages with access to food, ad libitum water. The upper Bavarian Government reviewed and approved all animal experiments and registered them under the 55.2-1-54-2532-16-61 and 55.2-2532-02-19-23 protocol. Unless otherwise stated, all animal experiments were conducted using 1-2 weeks old animals.

5.14 ShRNA Design and Plasmid Construction

To knock down the p120 expression, a distinct ShRNA sequence targeting mouse (5'CGA GGCTATGAACTCTTATTTCTCGAGAAATAAGAGTTCATAGCCTCG3') and a scrambled ShRNAsequence(5'CCTAAGGTTAAGTCGCCCTCGCTCGAGCGAGGGCGACTTAACCT TAGG 3`) was designed using Vector Biolabs (Malvern, PA). A U6 promoter was used to drive p120 ShRNA or scrambled ShRNA expression followed by green fluorescent protein (eGFP) separately driven by a CMV promoter. AAV U6-p120-shRNA plasmid was constructed, as shown in Figure 15A was purchased from Vector Biolabs (Malvern, PA). An AAV8 vector carrying either p120-shRNA or control ShRNA virus was made according to a three-plasmid co-transfection method described above.

5.15 *In Vivo* Injury Model and AAV Vector Injection

Two-week wildtype mice were anaesthetized with MMF (Medetomidine at 0.5 $mg.kg^{-1}$, midazolam at 5 $mg.kg^{-1}$, and fentanyl at 0.05 $mg.kg^{-1}$). Under analgesia, two deep wounds (i.e., epidermis, dermis, and fascia) were generated on the back skin. The mouse received an injection of 5µl of AAV-CMV-eGFP or AAV-CMV-Cre virus using a 33-gauge glass needle (Hamilton). Mice were carefully monitored daily for at least 1 week. After 7 days post-injury, the scar tissue was cryo-sectioned for histological and immunofluorescent analysis.

5.16 *Ex vivo* Live Imaging

Virus injected mice were sacrificed, and the wound region was collected in a prewarmed DMEM w/o phenol red supplemented with 10% KnockOut Serum,1% Penicillin/Streptomycin Antibiotics solution, 1% non-essential amino acids,1%L-glutamine. The tissue was embedded in 4 % agarose and agarose and submerged in a culture medium. The embedded tissue was transferred pre-equilibrated and humidified incubator chamber at 37 °C with a 5%

CO^2 atmosphere. Imaging was acquired using Leica SP8 multiphoton (MP) system with a tunable laser and LAS X software. Live imaging of AAV transduced GFP positive cells were acquired using 25X objective for 24h. Recorded z-stacks were converted into Imaris files using the ImarisFileConverterx64. The subsequent analyses were performed with Imaris (Version 9.1.0.X, Bitplane).

5.17 Matrix Labelling and AAV Injection in the Fascia

For the matrix labelling experiment, two-week-old wildtype mice (C57BL6/J) were injected with 5µl of FITC NHS ester subcutaneously. Prepare NHS-Flurescein solution of 10mg/ml in 0.1 M sodium bicarbonate buffer: pH9. The next day, 3mm deep wounds were generated on the FITC NHS ester labelled area. After the injury, the mice have subcutaneously injected with 10µl at titre range of $2x10^{12}$ GC/ml of AAV8 p120 ShRNA and AAV8 Control ShRNA virus at the wound region. After surgery, the mice were kept warm on the heating pad. After 7 days post wounding, immerse the tissue with 2% PFA and keep for overnight 4°C. The fixed samples were subjected to the sectioning and immunofluorescence staining.

5.18 Particle Image Velocimetry (PIV) Analysis

PIV analysis was performed using Fiji Plugin Iterative PIV`[104]. It compares the localisation of signals in 2 images and computes the pixel flow trajectories between them. Stable pictures from the timelapse devoid of tissue drifts from early and final time points were converted into a 2-picture stack to derive these trajectories. Images were converted to an 8-bit stack, and the "iterative PIV" function was applied. Default values with "Vector spacing" of 128, 64 and 32 pixels were applied, and trajectories and corresponding colour-ramps were exported as TIFFs.

5.19 Statistics

For 2 group comparisons, a two-tailed t-test (Student´s t-test) was carried out for the statistical analysis. The statistical analysis for all the comparisons was accomplished using GraphPad Prism 9.2. The Significant significance was presented in each figure legend.

REFERENCES

1. Gurtner GC, Werner S, Barrandon Y, Longaker MT. Wound repair and regeneration. Nature. 2008;453(7193):314-321.

2. Bayat A, McGrouther DA, Ferguson MW. Skin scarring. BMJ. 2003;326(7380):88-92.

3. Eming SA, Martin P, Tomic-Canic M. Wound repair and regeneration: Mechanisms, signaling, and translation. *Science Translational Medicine*. 2014;6(265).

4. Sheridan RL, Hinson MI, Liang MH, et al. Long-term Outcome of Children Surviving Massive Burns. *JAMA*. 2000;283(1):69-73.

5. PC E. Burn rehabilitation: an overview. *Archives of physical medicine and rehabilitation*. 2007;88(12 Suppl 2):S3.

6. Asuku ME, Ibrahim A, Ijekeye FO. Post-burn axillary contractures in pediatric patients: a retrospective survey of management and outcome. *Burns*. 2008;34(8):1190-1195.

7. Seifert J. Incidence and economic burden of injuries in the United States. *Journal of Epidemiology and Community Health*. 2007;61(10):926.

8. Hunt O, Burden D, Hepper P, Stevenson M, Johnston C. Self-reports of psychosocial functioning among children and young adults with cleft lip and palate. *Cleft Palate Craniofac J*. 2006;43(5):598-605.

9. Brown BC, McKenna SP, Siddhi K, McGrouther DA, Bayat A. The hidden cost of skin scars: quality of life after skin scarring. *J Plast Reconstr Aesthet Surg*. 2008;61(9):1049-1058.

10. Pasparakis M, Haase I, Nestle FO. Mechanisms regulating skin immunity and inflammation. Nat Rev Immunol. 2014;14(5):289-301.

11. Rousselle P, Braye F, Dayan G. Re-epithelialization of adult skin wounds: Cellular mechanisms and therapeutic strategies. *Advanced Drug Delivery Reviews*. 2019;146:344-365.

12. Rivera-Gonzalez G, Shook B, Horsley V. Adipocytes in Skin Health and Disease. *Cold Spring Harbor Perspectives in Medicine*. 2014;4(3).

13. Jiang D, Rinkevich Y. Furnishing Wound Repair by the Subcutaneous Fascia. Int J Mol Sci. 2021;22(16):9006.

14. Baum CL, Arpey CJ. Normal cutaneous wound healing: clinical correlation with cellular and molecular events. *Dermatologic surgery*. 2005;31(6):674-686.

15. Velnar T, Bailey T, Smrkolj V. The wound healing process: an overview of the cellular and molecular mechanisms. *The Journal of international medical research*. 2009;37(5):1528-1542.

16. Golebiewska EM, Poole AW. Platelet secretion: From haemostasis to wound healing and beyond. *Blood reviews*. 2015;29(3):153-162.

17. Zaidi, A. L. Green. Physiology of haemostasis. *Anaesthesia & Intensive Care Medicine*.2019 20,153-158.

18. Cognasse F, Hamzeh H, Chavarin P, Acquart S, Genin C, Garraud O. Evidence of Toll-like receptor molecules on human platelets. *Immunology and cell biology*. 2005;83(2):196-198.

19. Shiraki R, Inoue N, Kawasaki S, et al. Expression of Toll-like receptors on human platelets. *Thrombosis research*. 2004;113(6):379-385.

20. Tang YQ, Yeaman MR, Selsted ME. Antimicrobial peptides from human platelets. *Infection and immunity*. 2002;70(12):6524-6533.

21. Kolaczkowska E, Kubes P. Neutrophil recruitment and function in health and inflammation. *Nature reviews Immunology*. 2013;13(3):159-175.

22. Eming SA, Krieg T, Davidson JM. Inflammation in wound repair: molecular and cellular mechanisms. *The Journal of investigative dermatology*. 2007;127(3):514-525.

23. Rodero MP, Licata F, Poupel L, et al. In vivo imaging reveals a pioneer wave of monocyte recruitment into mouse skin wounds. *PLoS ONE*. 2014;9(10).

24. Engelhardt E, Toksoy A, Goebeler M, Debus S, Bröcker EB, Gillitzer R. Chemokines IL-8, GROalpha, MCP-1, IP-10, and Mig are sequentially and differentially expressed during phase-specific infiltration of leukocyte subsets in human wound healing. Am J Pathol. 1998;153(6):1849-1860

25. Delavary BM, van der Veer WM, van Egmond M, Niessen FB, Beelen RHJ. Macrophages in skin injury and repair. *Immunobiology*. 2011;216(7):753-762.

26. Driskell RR, Lichtenberger BM, Hoste E, et al. Distinct fibroblast lineages determine dermal architecture in skin development and repair. Nature. 2013;504(7479):277-281.

27. Lau K, Paus R, Tiede S, Day P, Bayat A. Exploring the role of stem cells in cutaneous wound healing. *Experimental Dermatology*. 2009;18(11):921-933.

28. Schultz GS, Wysocki A. Interactions between extracellular matrix and growth factors in wound healing. *Wound repair and regeneration.*2009;17(2):153-162.

29. Dallon JC, Ehrlich HP. A review of fibroblast-populated collagen lattices. *Wound Repair and Regeneration*. 2008;16(4):472-479.

30. Marshall CD, Hu MS, Leavitt T, Barnes LA, Lorenz HP, Longaker MT. Cutaneous Scarring: Basic Science, Current Treatments, and Future Directions. *Advances in Wound Care*. 2018;7(2):29-45.

31. Gabbiani G, Majno YG, Abercrombie IM, et al. Presence of modified fibroblasts in granulation tissue and their possible role in wound contraction. *Experientia 1971 27:5*. 1971;27(5):549-550.

32. Hinz B. Formation and function of the myofibroblast during tissue repair. *The Journal of investigative dermatology*. 2007;127(3):526-537.

33. Xue M, Jackson CJ. Extracellular Matrix Reorganization During Wound Healing and Its Impact on Abnormal Scarring. *Advances in Wound Care*. 2015;4(3):119-136.

34. van Zuijlen PP, Ruurda JJ, van Veen HA, et al. Collagen morphology in human skin and scar tissue: no adaptations in response to mechanical loading at joints. Burns. 2003;29(5):423-431.

35. Correa-Gallegos D, Jiang D, Christ S, et al. Patch repair of deep wounds by mobilized fascia. *Nature*. 2019;576(7786):287-292.

36. Wan L, Jiang D, Correa-Gallegos D, et al. Connexin43 gap junction drives fascia mobilization and repair of deep skin wounds. *Matrix Biology*. 2021;97:58-71.

37. Jiang D, Christ S, Correa-Gallegos D, et al. injury triggers fascia fibroblast collective cell migration to drive scar formation through N-cadherin. *Nature communications*. 2020;11(1).

38. Bayat A, McGrouther DA, Ferguson MWJ. Skin scarring. *BMJ.*2003;326(7380):88.

39. Peacock EE Jr, Madden JW, Trier WC. Biologic basis for the treatment of keloids and hypertrophic scars. *South Med J*. 1970;63(7):755-760.

40. Chen MA, Davidson TM. Scar management: prevention and treatment strategies. Curr Opin Otolaryngol Head Neck Surg. 2005;13(4):242-247.

41. Atkinson JA, McKenna KT, Barnett AG, McGrath DJ, Rudd M. A randomized, controlled trial to determine the efficacy of paper tape in preventing hypertrophic scar formation in surgical incisions that traverse Langer's skin tension lines. Plast Reconstr Surg. 2005;116(6):1648-1658.

42. Thomas JR, Somenek M. Scar Revision Review. *Archives of Facial Plastic Surgery*. 2012;14(3):162-174.

43. Jackson BA, Shelton AJ. Pilot study evaluating topical onion extract as treatment for postsurgical scars. *Dermatologic Surgery*. 1999;25(4):267-269.

44. Chowdri NA, Mattoo MMA, Darzi MA. Keloids and hypertrophic scars. *Australian and New Zealand Journal of Surgery*. 1999;69(9):655-659.

45. Ripper S, Renneberg B, Landmann C, Weigel G, Germann G. Adherence to pressure garment therapy in adult burn patients. *Burns : journal of the International Society for Burn Injuries*. 2009;35(5):657-664.

46. Kuo YR, Jeng SF, Wang FS, et al. Flashlamp pulsed dye laser (PDL) suppression of keloid proliferation through down-regulation of TGF-β1 expression and extracellular matrix expression. *Wiley Online Library*. 2004;34(2):104-108.

47. Poetschke J, Gauglitz GG. Current options for the treatment of pathological scarring. *JDDG: Journal der Deutschen Dermatologischen Gesellschaft*. 2016;14(5):467-477.

48. Malhotra AK, Gupta S, Khaitan BK, Sharma VK. Imiquimod 5% cream for the prevention of recurrence after excision of presternal keloids. Dermatology. 2007;215(1):63-65.

49. Denton CP, Merkel PA, Furst DE, et al. Recombinant human anti-transforming growth factor β1 antibody therapy in systemic sclerosis: A multicenter, randomized, placebo-controlled phase I/II trial of CAT-192. *Arthritis and Rheumatism*. 2007;56(1):323-333.

50. Prey S, Ezzedine K, Doussau A, et al. Imatinib mesylate in scleroderma-associated diffuse skin fibrosis: A phase II multicentre randomized double-blinded controlled trial. *British Journal of Dermatology*. 2012;167(5):1138-1144.

51. “Juvista (Avotermin) in Breast Reduction Surgery Scars - Full Text View - clinicaltrials.gov.” https://clinicaltrials.gov/ct2/show/NCT00432328.

52. “A Clinical Study of Allogeneic Human Dermal Fibroblasts for Remodeling Scar Contractures.” https://clinicaltrials.gov/ct2/show/study/NCT01564407.

53. Galiano RD, Jewell ML, Jensen J, et al. An Antisense Oligonucleotide (EXC 001) Targeting Connective Tissue Growth Factor Reduces Skin Scarring Associated with Abdominoplasty and Reduces CTGF Expression. *Plastic and Reconstructive Surgery*. 2011;128:45.

54. Atchison RW, Casto BC, Hammon WMD. Adenovirus-Associated Defective Virus Particles. *Science.* 1965;149(3685):754-756.

55. Im DS, Muzyczka N. Partial purification of adeno-associated virus Rep78, Rep52, and Rep40 and their biochemical characterization. *Journal of virology*. 1992;66(2):1119-1128.

56. Becerra SP, Rose JA, Hardy M, Baroudy BM, Anderson CW. Direct mapping of adeno-associated virus capsid proteins B and C: a possible ACG initiation codon. *Proceedings of the National Academy of Sciences of the United States of America*. 1985;82(23):7919.

57. Trempe JP, Carter BJ. Alternate mRNA splicing is required for synthesis of adeno-associated virus VP1 capsid protein. *Journal of Virology*. 1988;62(9):3356-3363.

58. Naumer M, Sonntag F, Schmidt K, et al. Properties of the adeno-associated virus assembly-activating protein. *Journal of virology*. 2012;86(23):13038-13048.

59. Duan D, Li Q, Kao AW, Yue Y, Pessin JE, Engelhardt JF. Dynamin is required for recombinant adeno-associated virus type 2 infection. *Journal of virology*. 1999;73(12):10371-10376.

60. Bartlett JS, Wilcher R, Samulski RJ. Infectious entry pathway of adeno-associated virus and adeno-associated virus vectors. *Journal of virology*. 2000;74(6):2777-2785.

61. Grimm D, Kay MA, Kleinschmidt JA. Helper virus-free, optically controllable, and two-plasmid-based production of adeno-associated virus vectors of serotypes 1 to 6. *Molecular therapy*. 2003;7(6):839-850.

62. Grimm D, Kern A, Rittner K, Kleinschmidt JA. Novel tools for production and purification of recombinant adenoassociated virus vectors. *Human gene therapy*. 1998;9(18):2745-2760.

63. Xiao X, Li J, Samulski RJ. Production of high-titer recombinant adeno-associated virus vectors in the absence of helper adenovirus. *Journal of virology*. 1998;72(3):2224-2232.

64. Ferrari FK, Samulski T, Shenk T, Samulski RJ, Center GT. Second-strand synthesis is a rate-limiting step for efficient transduction by recombinant adeno-associated virus vectors. *Journal of Virology*. 1996;70(5):3227.

65. Fisher KJ, Gao GP, Weitzman MD, Dematteo R, Burda JF, Wilson JM. Transduction with recombinant adeno-associated virus for gene therapy is limited by leading-strand synthesis. *Journal of Virology*. 1996;70(1):520.

66. McCarty DM. Self-complementary AAV Vectors; Advances and Applications. *Molecular Therapy*. 2008;16(10):1648-1656.

67. McCarty DM, Monahan PE, Samulski RJ. Self-complementary recombinant adeno-associated virus (scAAV) vectors promote efficient transduction independently of DNA synthesis. *Gene Therapy 2001 8:16*. 2001;8(16):1248-1254.

68. Choi V, McCarty D, Samulski R. AAV hybrid serotypes: improved vectors for gene delivery. *Current gene therapy*. 2005;5(3):299-310.

69. Deodato B, Arsic N, Zentilin L, et al. Recombinant AAV vector encoding human VEGF165 enhances wound healing. *Gene therapy*. 2002;9(12):777-785.

70. Galeano M, Deodato B, Altavilla D, et al. Adeno-associated viral vector-mediated human vascular endothelial growth factor gene transfer stimulates angiogenesis and wound healing in the genetically diabetic mouse. *Diabetologia*. 2003;46(4):546-555.

71. Braun-Falco M, Doenecke A, Smola H, Hallek M. Efficient gene transfer into human keratinocytes with recombinant adeno-associated virus vectors. *Gene therapy*. 1999;6(3):432-441.

72. Gagnoux-Palacios L, Hervouet C, Spirito F, et al. Assessment of optimal transduction of primary human skin keratinocytes by viral vectors. *The Journal of Gene Medicine*. 2005;7(9):1178-1186.

73. Keswani SG, Balaji S, Le L, et al. Pseudotyped adeno-associated viral vector tropism and transduction efficiencies in murine wound healing. *Wound repair and regeneration*. 2012;20(4):592-600.

74. Hengge UR, Mirmohammadsadegh A. Adeno-associated virus expresses transgenes in hair follicles and epidermis. *Molecular therapy.*2000;2(3):188-194.

75. Taulet N, Comunale F, Favard C, Charrasse S, Bodi S, Gauthler-Rouvière C. N-cadherin/p120 Catenin Association at Cell-Cell Contacts Occurs in Cholesterol-rich Membrane Domains and Is Required for RhoA Activation and Myogenesis. *Journal of Biological Chemistry*. 2009;284(34):23137-23145.

76. Darzi MA, Chowdri NA, Kaul SK, Khan M. Evaluation of various methods of treating keloids and hypertrophic scars: a 10-year follow-up study. Br J Plast Surg. 1992 Jul;45(5):374-9.

77. Berman B, Kaufman J. Pilot study of the effect of postoperative imiquimod 5% cream on the recurrence rate of excised keloids. *J Am Acad Dermatol*. 2002 Oct;47(4 Suppl):S209-11

78. Saulis AS, Mogford JH, Mustoe TA. Effect of Mederma on hypertrophic scarring in the rabbit ear model. *Plast Reconstr Surg*. 2002 Jul;110(1):177-83

79. Atiyeh BS, Amm CA, el Musa KA. Improved Scar Quality Following Primary and Secondary Healing of Cutaneous Wounds. *Aesthetic Plastic Surgery*. 2003;27(5):411-417.

80. Pillay S, Meyer NL, Puschnik AS, et al. An essential receptor for adeno-associated virus infection. *Nature* 2016 *530:7588*. 2016;530(7588):108-112.

81. Kotterman MA, Schaffer D v. Engineering adeno-associated viruses for clinical gene therapy. *Nature reviews Genetics*. 2014;15(7):445-451.

82. Basner-Tschakarjan E, Mingozzi F. Cell-Mediated Immunity to AAV Vectors, Evolving Concepts and Potential Solutions. *Frontiers in Immunology*. 2014;0(JUL):350.

83. Kourtidis A, Ngok SP, Anastasiadis PZ. p120 catenin: an essential regulator of cadherin stability, adhesion-induced signaling, and cancer progression. *Progress in molecular biology and translational science*. 2013;116:409.

84. Grosheva I, Shtutman M, Elbaum M, Bershadsky AD. p120 catenin affects cell motility via modulation of activity of Rho-family GTPases: a link between cell-cell contact formation and regulation of cell locomotion. *Journal of Cell Science*. 2001;114(4):695-707.

85. Tseng Q, Duchemin-Pelletier E, Deshiere A, et al. Spatial organization of the extracellular matrix regulates cell-cell junction positioning. *Proceedings of the National Academy of Sciences of the United States of America*. 2012;109(5):1506-1511.

LIST OF ABBREVIATIONS

- **AAV** Adeno Associated Virus
- **PDGF** Platelet-Derived Growth Factor
- **IL-8** Interleukin 8
- **TNF** Tumour Necrosis Factor
- **ECM** Extracellular Matrix
- **MCP-1** Monocyte Chemoattractant Protein-1
- **VEGF** Vascular Endothelial Growth Factor
- **CD90** Cluster of Differentiation 90
- **FSP-1** Fibroblast-Specific Protein 1
- **α-SMA** Alpha-Smooth Muscle Actin
- **EPF** Engrailed-1 Positive Fibroblasts
- **CTGF** Connective Tissue Growth Factor
- **WT** Wild Type
- **ORF** Open Reading Frames
- **ITR** Inverted Terminal Repeats
- **AAP** Assembly-Activating Protein
- **HSPG** Heparan Sulfate Proteoglycan
- **EGFR** Epidermal Growth Factor Receptor
- **HGFR** Hepatocyte Growth Factor Receptor
- **FGFR1** Fibroblast Growth Factor Receptor 1
- **CNS** Central Nervous System
- **LamR** Laminin Receptor
- **TGF-β** Transforming Growth Factorβ.
- **eGFP** enhanced Green Fluorescent Protein
- **ShRNA** Short hairpin RNA
- **Kb** Kilobase
- **scAAV** Self-complementary Adeno Associated Virus
- **dpw** days post wounding
- **DMEM** Dulbecco's Modified Eagle Medium
- **FCS** Fetal Calf Serum
- **PIV** Particle Image Velocimetry
- **PFA** Paraformaldehyde

LIST OF PUBLICATIONS AND CONTRIBUTIONS

1) **Rajendran V**, Ramesh P, Kalgudde Gopal S,Ye H, Rinkevich Y. **Therapeutic silencing of p120 in fascia fibroblasts induces scarless wound repair**. (Manuscript in preparation)

2) Jiang D, Correa-Gallegos D, Christ S, Stefanska A, Liu J, Ramesh P, **Rajendran V**, De Santis MM, Wagner DE, Rinkevich Y. **Two succeeding fibroblastic lineages drive dermal development and the transition from regeneration to scarring**. Nat Cell Biol. 2018 Apr;20(4):422-431. doi: 10.1038/s41556-018-0073-8. Epub 2018 Mar 28. PMID: 29593327.

3) Jiang D, Christ S, Correa-Gallegos D, Ramesh P, Kalgudde Gopal S, Wannemacher J, Mayr CH, Lupperger V, Yu Q, Ye H, Mück-Häusl M, **Rajendran V**, Wan L, Liu J, Mirastschijski U, Volz T, Marr C, Schiller HB, Rinkevich Y. **Injury triggers fascia fibroblast collective cell migration to drive scar formation through N-cadherin.** Nat Commun. 2020 Nov 6;11(1):5653. doi: 10.1038/s41467-020-19425-1. PMID: 33159076.

4) Feng W, Kawauchi D, Körkel-Qu H, Deng H, Serger E, Sieber L, Lieberman JA, Jimeno-González S, Lambo S, Hanna BS, Harim Y,Jansen M, Neuerburg A, Friesen O, Zuckermnn M, **Rajendran V**, Gronych J, Ayrault O, Korshunov A, Jones DT, Kool M, Northcott PA, Lichter P, Cortés-Ledesma F, Pfister SM, Liu HK. **Chd7 is indispensable for mammalian brain development through activation of a neuronal differentiation programme**. Nat Commun. 2017 Mar 20;8:14758. doi: 10.1038/ncomms14758. PMID: 28317875; PMCID: PMC5364396.

ACKNOWLEDGMENTS

I am incredibly thankful to my direct supervisor, **Dr Yuval Rinkevich**, for performing my PhD in his group. I am grateful for your guidance, enthusiasm, and great ideas for my project. Importantly, I am very much thankful for all the scientific knowledge I got from you.

I would also extend my heartful thanks to my second supervisor **PD Dr Claudia Staab-Weijnitz,** has been immensely supportive throughout my PhD. Thanks for all the research school training, and knowledge throughout my PhD days.

My sincere thanks to **Prof. Dr Maria Elena Torres-Padilla** to be a part of my TAC meetings and for fruitful discussions and suggestions on my project. Moreover, I would like to thank all the members of the doctoral thesis committee for refereeing my thesis.

I extend my thankfulness to all the Comprehensive Pneumology Center (CPC) and Institute of Lung Biology and Disease (ILBD) crew. In addition, I would like to thank the SMAP team and Unit34, LMU Bio-imaging core facility, for their invaluable support in this project

Special Thanks to Sandra for taking care of all the administrative work. I am always grateful for all the support you provided.

My completion of this project could not have been accomplished without the support of the entireRinkevich Lab members. Thanks for all the help.

A great and warm thanks to all the coffee dudes: Aydan, Shruthi, Pushkar, Ashesh, Ceylan, Tim, Haifeng, Andy, Michal, Valeria, Ruoxuan, Johannes, Tankut. I had a lot of fun with you guys. I wish you all very good luck in the next phase of your career. I would like to thank Thiru, we have been friends for more than a decade and it´s amazing how time flies. I enjoyed all the scientific, and political discussions that we had. I wish you good luck for the next part of your life.

Finally, I extend my sincere gratitude to my family for being a driving factor to complete this journey.

LMU LUDWIG-MAXIMILIANS-UNIVERSITÄT MÜNCHEN

Dean's Office
Medical Faculty

MMRS

Affidavit

Rajendran, Vijayanand
_____
Surname, first name

Germany
_____
Country

I hereby declare that the submitted thesis entitled:

Harnessing Adeno Associated Virus (AAV) Technology for the Treatment of Scarring

is my own work. I have only used the sources indicated and have not made unauthorised use of services of a third party. Where the work of others has been quoted or reproduced, the source is always given.

I further declare that the dissertation presented here has not been submitted in the same or similar form to any other institution for the purpose of obtaining an academic degree.

Munich, 17.06.2022 Vijayanand Rajendran

_____ _____

place, date Signature doctoral candidate

LMU LUDWIG-MAXIMILIANS-UNIVERSITÄT MÜNCHEN

Dean's Office
Medical Faculty

MMRS

Confirmation of congruency between printed and electronic version of the doctoral thesis

Rajendran, Vijayanand

Surname, first name

Germany

Country

I hereby declare that the submitted thesis entitled:

Harnessing Adeno Associated Virus (AAV) Technology for the Treatment of Scarring

…….

is congruent with the printed version both in content and format.

Munich, 17.06.2022 Vijayanand Rajendran

place, date Signature doctoral candidate